EURASIP Journal on Wireless Communications and Networking

RESEARCH Open Access

Jointly optimized design of distributed RS-coded spatial modulation by appropriate selection at the relay

Chunli Zhao[1*], Fengfan Yang[1], Waheed Ullah[2] and Pengcheng Guo[1]

*Correspondence:
chunlizhao_cn@163.com

[1] College of Electronic and Information Engineering, Nanjing University of Aeronautics and Astronautics, Nanjing 210016, China
[2] School of Electrical and Information Engineering, University of the Witwatersrand, Johannesburg 2000, South Africa

Abstract

This paper proposes the distributed Reed–Solomon (RS)-coded spatial modulation (DRSC-SM) scheme over quasi-static Rayleigh fading channel. Two different RS codes are used, one having a smaller minimum distance at the source and the other having a larger minimum distance at the relay. In order to obtain an optimized code at the destination, a proper encoding strategy must be adapted at the relay. Thus, an efficient design approach is proposed that suitably selects the symbols at the relay. Using this optimized approach as a benchmark, another design is proposed to achieve reduced complexity. To jointly decode the source and relay RS codes, three different decoding algorithms known as the naive, smart and improved smart algorithms are presented. Monte Carlo simulated results reveal that the proposed DRSC-SM scheme utilizing the improved smart decoding algorithm outperforms its counterpart DRSC-SM scheme employing the naive and smart decoding algorithms under identical conditions. The simulation results also validate the superiority of the proposed DRSC-SM scheme over its corresponding coded noncooperative scheme under the same decoding algorithm.

Keywords: RS codes, Coded cooperation, SM, Joint RS decoding

1 Introduction

Multiple-input multiple-output (MIMO) systems have been recognized as a core technique for improving the spectral efficiency and link reliability comparing with single antenna wireless systems [1]. A well-known MIMO technique is the vertical Bell Labs Layered Space-Time (V-BLAST) architecture. However, simultaneously transmitting multiple independent data streams from all the antennas requires inter-antenna synchronization (IAS) [2]. The V-BLAST scheme also suffers from inter-channel interference (ICI) at the receiver. Spatial modulation (SM) is able to avoid these problems [3]. This is because only one active transmit antenna is used by SM to transmit constellation symbol at each time instant. Moreover, the utilization of the transmit antenna index as an information-bearing unit effectively boosts the spectral efficiency.

Recently, coded cooperative diversity has drawn substantial research efforts as an efficient technique to combat channel fading, which is an integration of channel codes and cooperative diversity techniques like compress-and-forward (CF), decode-and-forward

Springer Open

© The Author(s) 2023. **Open Access** This article is licensed under a Creative Commons Attribution 4.0 International License, which permits use, sharing, adaptation, distribution and reproduction in any medium or format, as long as you give appropriate credit to the original author(s) and the source, provide a link to the Creative Commons licence, and indicate if changes were made. The images or other third party material in this article are included in the article's Creative Commons licence, unless indicated otherwise in a credit line to the material. If material is not included in the article's Creative Commons licence and your intended use is not permitted by statutory regulation or exceeds the permitted use, you will need to obtain permission directly from the copyright holder. To view a copy of this licence, visit http://creativecommons.org/licenses/by/4.0/.

(DF) and amplify-and-forward (AF) [4–6]. To attain coded cooperative diversity, various distributed channel codes like distributed polar codes [7], distributed low-density parity-check (LDPC) codes [8], distributed Reed–Muller (RM) codes [4] and distributed turbo codes [9] have been proposed. The information theoretical analysis has corroborated that coded cooperative scheme achieves a better bit error rate (BER) performance as compared to its counterpart noncooperative scheme. Many related works about distributed channel codes have been studied to achieve coded cooperation. However, less research in the literature is available on the idea of subcode at the destination to enhance system performance through improving the minimum distance.

The 5G communication will require to support traffic originated by devices (usually sensors and actuators) and machines which are involved in communications such as machine-to-machine (M2M) or device-to-device (D2D) communication [10, 11]. Usually, the information sequences with the short length are required in the 5G communication. The well-known short-length RS codes possess simple encoding and decoding complexity, and are very effective in correcting random symbol errors and random burst errors. As maximum distance separable (MDS) codes [12], the short-length RS codes with simple encoding and decoding complexity are able to obtain the superior error performance as well, which shows that the short RS codes can achieve a trade-off between the complexity and error performance. Therefore, the short-length RS codes may be considered as a powerful candidate in 5G scenarios such as ultra-reliable and low-latency communications (URLLC).

In recent literature works [13–15], the short RS codes were distributed effectively to construct the coded cooperative networks, which can offer reasonable BER performance with low encoding and decoding complexity. In [1, 5], the authors have introduced that the amalgamation of existing MIMO techniques with the cooperative techniques promises to enhance the spectral efficiency. Thus, in this paper, an emerging MIMO technique, i.e., SM is incorporated into the distributed RS coding scheme, and the distributed RS-coded SM (DRSC-SM) scheme is proposed.

In our proposed DRSC-SM scheme, the source and relay employ different RS codes. At the relay, the information symbols are chosen out of the source transmitted signal. By the mutual cooperation between source and relay, the jointly constructed code is generated at the destination. The closest work related to our paper is presented in [16] where the relay selects the partial information symbols from the decoded source information symbols by the random selection pattern so that a code resulted by the random selection is generated at the destination. However, our paper uses an efficient approach to get the optimized selection pattern by which partial information symbols are properly selected at the relay in order to achieve the optimized code at the destination. Considering this approach as a benchmark, another reduced complexity approach is employed. Our paper also proposes an improved smart decoding algorithm different from the decoding algorithms in [16] to jointly recover the source information. Moreover, the utilization of SM and the improved smart algorithm makes our proposed scheme be very distinct from the recently published literature [17]. The main contributions of this paper are as follows:

- DRSC-SM scheme through quasi-static Rayleigh fading channel is proposed.

- An efficient approach for selecting proper symbols at the relay node is proposed to produce optimized code at the destination.
- Another approach with reduced complexity for constructing the optimized code at the destination is also developed.
- At the destination, the joint RS decoding is used in DRSC-SM system with three decoding algorithms known as the naive algorithm, smart algorithm and improved smart algorithm.

The remaining paper is organized as follows. Section 2 introduces the general design of distributed linear block coded SM by subspace approach. Section 3 presents the system model of DRSC-SM scheme. In Sect. 4, the jointly optimized design for DRSC-SM scheme is presented. Section 5 introduces the joint RS decoding with three different decoding algorithms. Section 6 presents the simulation results. Finally, Sect. 7 concludes this article.

2 General design of distributed linear block coded SM by subspace approach

In this section, a general design of distributed linear block coded SM by subspace approach is discussed. The following two subsections explain the general design in detail.

2.1 Distributed linear block codes by subspace approach

A basic coded cooperative communication scheme includes three nodes such as source node (S), relay node (R) and destination node (D) as illustrated in Fig. 1. The DF relaying protocol is employed in cooperative scheme. It requires two time slots to complete the whole communication transmission. In time slot 1, the source node encodes information sequence $\mathbf{m}_1$ of length K_1 into codeword $\mathbf{c}_1$ of length N using the linear block code $C_1(N, K_1)$, and broadcasts the modulated sequence toward relay and destination nodes.

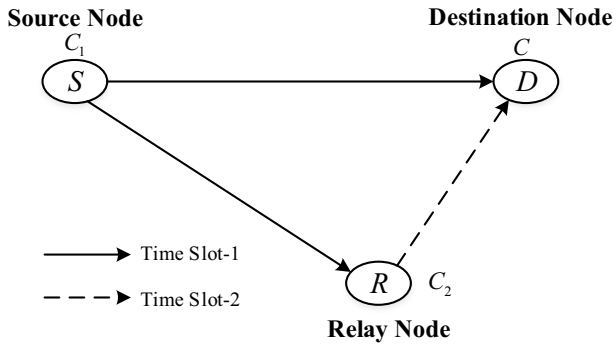

Fig. 1 General system model of distributed linear block codes. It requires two time slots to complete the whole communication transmission, where solid and dashed lines denote the first and second time slots, respectively. The source and relay nodes have linear block codes C_1 and C_2, respectively, which are distributed to achieve coded cooperation. The resulted code at the destination is $C = \{|\mathbf{c}_1|\mathbf{c}_2|, \mathbf{c}_1 \in C_1, \mathbf{c}_2 \in C_2\}$. Since no additional information is generated at the relay (the information at the relay depends on the information at the source) in our proposed system model, the code C is a subcode of $\bar{C} = \{|\mathbf{c}_1|\bar{\mathbf{c}}_2|, \mathbf{c}_1 \in C_1, \bar{\mathbf{c}}_2 \in C_2\}$, where $\bar{\mathbf{c}}_2$ corresponds to the information independent on the information at the source

In time slot 2, a part of decoded source transmission sequence $\widetilde{\mathbf{m}}_1$, that is, $\mathbf{m}_2$ of length $K_2(K_2 < K_1)$ is encoded into $\mathbf{c}_2$ of length N using $C_2(N, K_2)$ at the relay. Note that $\widetilde{\mathbf{m}}_1$ may not be equal to $\mathbf{m}_1$ due to the noisy $S - R$ channel link. However, without additional statement, it is assumed $\widetilde{\mathbf{m}}_1 = \mathbf{m}_1$ for notational convenience. The codes $C_1(N, K_1)$ and $C_2(N, K_2)$ are distributed to achieve coded cooperation, where $C_1(N, K_1)$ and $C_2(N, K_2)$ have minimum distances denoted as d_1 and d_2, respectively.

If the relay node encodes the additional K_2 information symbols $\bar{\mathbf{m}}_2$ independent of information sequence $\mathbf{m}_1$ into the codeword $\bar{\mathbf{c}}_2 \in C_2(N, K_2)$, then by concatenating $\mathbf{c}_1$ and $\bar{\mathbf{c}}_2$ the linear block code $\bar{C} = \{|\mathbf{c}_1|\bar{\mathbf{c}}_2|, \mathbf{c}_1 \in C_1(N, K_1), \bar{\mathbf{c}}_2 \in C_2(N, K_2)\}$ with the minimum distance $d_{\min}(\bar{C}) = d_1$ is resulted at the destination. However, no extra information symbols are resulted in the relay in our investigated distributed linear block coding scheme since all the information symbols $\mathbf{m}_2$ depend on $\mathbf{m}_1$. The resulted code at the destination is $C = \{|\mathbf{c}_1|\mathbf{c}_2|, \mathbf{c}_1 \in C_1(N, K_1), \mathbf{c}_2 \in C_2(N, K_2)\}$, which is the subcode of code $\bar{C}$, i.e., $C \in \bar{C}$.

2.2 Distributed channel coding combined with SM

Coded cooperative communication takes advantage of broadcast nature of the wireless medium to enhance the performance of transmission, which is a valid way that resists channel impairment and shadowing, and enlarges network coverage. Since future wireless communications have a demand for high spectral efficiency and high data rates, further boosting spectral efficiency and data rates of coded cooperation is very pivotal.

MIMO techniques are promising candidates in wireless networks to enhance data rates. By exploiting multiple antennas to transmit data simultaneously, the spectral efficiency is boosted. Many available studies have also presented that incorporating MIMO techniques into the cooperative communication can enhance spectral efficiency, improve data rates and extend network coverage. SM is a recently developed MIMO technique. At any time instant, only one transmit antenna is activated to transmit the constellation symbol. An important feature is that the transmit antenna index is an added source of information. Thus, there are many advantages using SM. For example, ICI and IAS can be completely avoided. Furthermore, the system complexity can be greatly reduced, which is because only activating one transmit antenna at each time instant implies that only one radio-frequency (RF) chain is required. Also, the use of SM provides the spatial diversity for the system. Moreover, the spectral efficiency can be efficiently enhanced due to the utilization of the transmit antenna index as an information-bearing unit. These attractive characteristics make SM be applied in the distributed channel coding scheme by subspace approach.

The earlier section has discussed that short-length non-binary RS codes are a special type of MDS code. Moreover, short-length RS codes can reach singleton bound and have an ability to correct random burst errors, and are then used for distributed channel codes combined with SM to perform error control. The specific system model of distributed RS-coded SM scheme is presented in the next section.

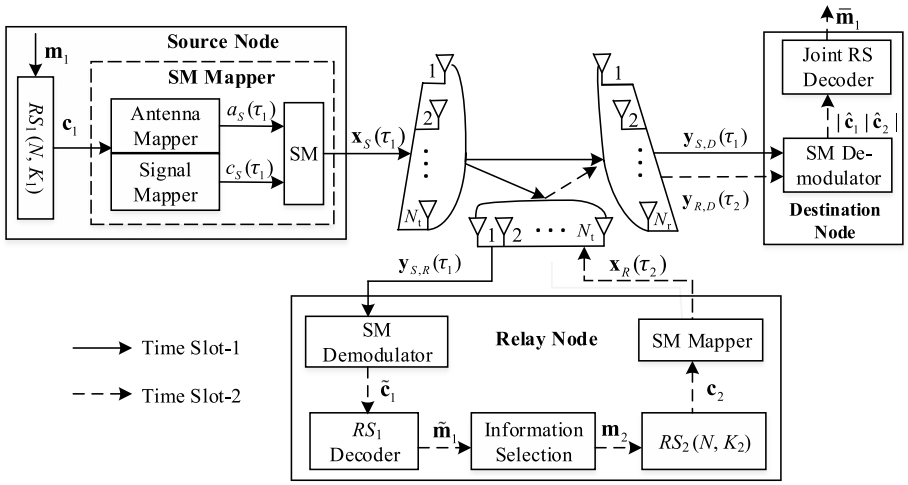

Fig. 2 DRSC-SM scheme for cooperative communications. The source *S*, relay *R* and destination *D* are equipped with N_t, N_t and N_r antennas, respectively. The RS codes RS_1 and RS_2 are employed at the source and relay nodes, respectively. During time slot 1, the source node encodes the information sequence $\mathbf{m}_1$ into codeword $\mathbf{c}_1$, which is given into SM mapper. The generated transmission vector is then sent to relay and destination nodes. During time slot 2, the demodulated codeword by the SM demodulator at the relay node is fed into the RS_1 decoder to generate the estimated information sequence. After the RS_2 encoder, the codeword $\mathbf{c}_2$ is generated and further sent to the SM mapper. Then, the generated transmission vector at the relay is sent to destination node. At the common destination node, the SM demodulator demodulates the received vectors during their time slots. Finally, the joint RS decoder is performed to jointly decode the source and relay signal

3 System model of distributed RS-coded SM scheme

The system model of distributed RS-coded SM (DRSC-SM) scheme is illustrated in Fig. 2, where the source *S*, relay *R* and destination *D* are equipped with N_t, N_t and N_r antennas, respectively. Completing an entire communication transmission requires two time slots.

In time slot 1, the source utilizes RS code $RS_1(N, K_1)$ of dimension K_1 and length N over GF(2^n) $(n = 1, 2, \cdots)$ to encode the non-binary information sequence $\mathbf{m}_1$, where each element in GF(2^n) can be denoted as a binary vector with length n. The RS code RS_1 has code rate $R_1 = K_1/N$ and generator polynomial $\mathbf{g}_1(X) = (X - \beta)(X - \beta^2)\cdots(X - \beta^{N-K_1})$, where $\beta^{f_1} \in$ GF(2^n) are the roots of $\mathbf{g}_1(X)$ for $f_1 \in \{1, 2, \cdots, N - K_1\}$. Then, the codeword polynomial $\mathbf{c}_1(X)$ of systematic codeword $\mathbf{c}_1$ is expressed as

$$\mathbf{c}_1(X) = X^{N-K_1}\mathbf{m}_1(X) + \mathbf{p}_1(X) \tag{1}$$

where the expression $\mathbf{m}_1(X) = m_0^{(1)} + m_1^{(1)}X + \cdots + m_{K_1-1}^{(1)}X^{K_1-1}$ with $m_{i_1}^{(1)} \in$ GF(2^n $)(i_1 = 0, 1, \cdots, K_1 - 1)$ is the polynomial representation of message sequence $\mathbf{m}_1$, and $\mathbf{c}_1(X) = c_0^{(1)} + c_1^{(1)}X + \cdots + c_{N-1}^{(1)}X^{N-1}$ with $c_{l_1}^{(1)} \in$ GF(2^n)$(l_1 = 0, 1, \cdots, N - 1)$. Furthermore, $\mathbf{p}_1(X) = p_0^{(1)} + p_1^{(1)}X + \cdots + p_{N-K_1-1}^{(1)}X^{N-K_1-1}$ having $p_{\zeta_1}^{(1)} \in$ GF(2^n $)(\zeta_1 = 0, 1, \cdots, N - K_1 - 1)$ is the parity polynomial and can be computed using polynomial division in GF(2^n) such as

$$\mathbf{p}_1(X) = X^{N-K_1}\mathbf{m}_1(X)/\mathbf{g}_1(X) \tag{2}$$

The codeword polynomial $\mathbf{c}_1(X)$ can be represented in sequence form, i.e., $\mathbf{c}_1 = [c_0^{(1)}, c_1^{(1)}, \cdots, c_{N-1}^{(1)}] = [\mathbf{p}_1, \mathbf{m}_1]$, where the expressions $\mathbf{p}_1 = [p_0^{(1)}, p_1^{(1)}, \cdots, p_{N-K_1-1}^{(1)}]$ and $\mathbf{m}_1 = [m_0^{(1)}, m_1^{(1)}, \cdots, m_{K_1-1}^{(1)}]$ are the parity and message symbol sequences, respectively. Since RS code is a non-binary MDS code, the minimum distance of RS code RS_1 is exactly expressed as $d_1 = N - K_1 + 1$. In the following, the binary vector $\mathbf{c}' = [c'_0, c'_1, \cdots, c'_{n-1}]$ representation for each codeword symbol $c_{l_1}^{(1)}$ is partitioned into two parts. The first $n_a = \log_2(N_\mathrm{t})$ bits of $\mathbf{c}'$ are given into the antenna mapper to select one active transmit antenna index labeled by $a_S(\tau_1) \in \{1, 2, \ldots, N_\mathrm{t}\}$, where $\tau_1 \in \{0, 1, \cdots, N-1\}$. The remaining $n_c = n - n_a = \log_2(M)$ bits are sent to the signal mapper that outputs an M-QAM/PSK modulated symbol $c_S(\tau_1) \in \Lambda$ with Λ being the signal constellation. Through SM, the modulated symbol $c_S(\tau_1)$ is transmitted at the $a_S(\tau_1)$th antenna, and the transmission vector $\mathbf{x}_S(\tau_1) = [\cdots, 0, c_S(\tau_1), 0, \cdots]^T$ is generated, where $[\cdot]^T$ denotes the transpose of a vector or matrix. For illustration, Table 1 exhibits different mapping results of SM scheme with code over GF(2^4), where the product of N_t and M is equal to 16, i.e., $MN_\mathrm{t} = 16$. In Table 1, the notation α is a primitive element of GF(2^4). Accordingly, $\alpha^{-\infty} \triangleq 0, \alpha^0 = 1, \alpha, \cdots, \alpha^{14}$ constitute all the elements of GF(2^4). In fact, various finite fields possess different communication scenarios under various combinations of N_t and M. These communication scenarios with RS code over GF(2^3), GF(2^4),GF(2^5) and GF(2^6) are given in Table 2, respectively. At the relay and destination nodes, the received signals $\mathbf{y}_{S,R}(\tau_1)$ and $\mathbf{y}_{S,D}(\tau_1)$ are separately mathematically written as

$$\begin{aligned}\mathbf{y}_{S,R}(\tau_1) &= \mathbf{H}_{S,R}\mathbf{x}_S(\tau_1) + \mathbf{n}_{S,R}(\tau_1) \\ &= \mathbf{h}_{S,R}^{a_S(\tau_1)} c_S(\tau_1) + \mathbf{n}_{S,R}(\tau_1)\end{aligned} \tag{3}$$

Table 1 Different mapping results of SM scheme with code over GF(2^4)

Field elements	Binary vector	$N_\mathrm{t} = 2$,8-QAM Antenna index, modulated symbol	$N_\mathrm{t} = 4$,4-QAM Antenna index, modulated symbol	$N_\mathrm{t} = 8$,BPSK Antenna index, modulated symbol
0	(0 0 0 0)	$(1, -3 + i)$	$(1, -1 - i)$	$(1, -1)$
1	(1 0 0 0)	$(2, -3 + i)$	$(3, -1 - i)$	$(5, -1)$
α	(0 1 0 0)	$(1, 3 + i)$	$(2, -1 - i)$	$(3, -1)$
α^2	(0 0 1 0)	$(1, -1 + i)$	$(1, 1 - i)$	$(2, -1)$
α^3	(0 0 0 1)	$(1, -3 - i)$	$(1, -1 + i)$	$(1, 1)$
α^4	(1 1 0 0)	$(2, 3 + i)$	$(4, -1 - i)$	$(7, -1)$
α^5	(0 1 1 0)	$(1, 1 + i)$	$(2, 1 - i)$	$(4, -1)$
α^6	(0 0 1 1)	$(1, -1 - i)$	$(1, 1 + i)$	$(2, 1)$
α^7	(1 1 0 1)	$(2, 3 - i)$	$(4, -1 + i)$	$(7, 1)$
α^8	(1 0 1 0)	$(2, -1 + i)$	$(3, 1 - i)$	$(6, -1)$
α^9	(0 1 0 1)	$(1, 3 - i)$	$(2, -1 + i)$	$(3, 1)$
α^{10}	(1 1 1 0)	$(2, 1 + i)$	$(4, 1 - i)$	$(8, -1)$
α^{11}	(0 1 1 1)	$(1, 1 - i)$	$(2, 1 + i)$	$(4, 1)$
α^{12}	(1 1 1 1)	$(2, 1 - i)$	$(4, 1 + i)$	$(8, 1)$
α^{13}	(1 0 1 1)	$(2, -1 - i)$	$(3, 1 + i)$	$(6, 1)$
α^{14}	(1 0 0 1)	$(2, -3 - i)$	$(3, -1 + i)$	$(5, 1)$

Table 2 Different communication scenarios with RS code over various Galois fields

Finite field	N_t	M
GF(2^3)	2	4
	4	2
GF(2^4)	2	8
	4	4
	8	2
GF(2^5)	2	16
	4	8
	8	4
	16	2
GF(2^6)	2	32
	4	16
	8	8
	16	4
	32	2

$$\begin{aligned}\mathbf{y}_{S,D}(\tau_1) &= \mathbf{H}_{S,D}\mathbf{x}_S(\tau_1) + \mathbf{n}_{S,D}(\tau_1)\\ &= \mathbf{h}_{S,D}^{a_S(\tau_1)} c_S(\tau_1) + \mathbf{n}_{S,D}(\tau_1)\end{aligned} \tag{4}$$

where $\mathbf{H}_{S,R}$ and $\mathbf{n}_{S,R}(\tau_1)$ in (3) separately denote the $N_t \times N_t$ channel matrix and $N_t \times 1$ noise vector, and their entries separately follow complex Gaussian distribution $CN(0, 1)$ and $CN(0, N_0)$ with N_0 being the noise power spectral density. $\mathbf{H}_{S,D}$ and $\mathbf{n}_{S,D}(\tau_1)$ in (4) are defined like $\mathbf{H}_{S,R}$ and $\mathbf{n}_{S,R}(\tau_1)$ in (3), respectively. Furthermore, $\mathbf{h}_{S,R}^{a_S(\tau_1)}$ and $\mathbf{h}_{S,D}^{a_S(\tau_1)}$ stand for the $a_S(\tau_1)$th columns of channel matrices $\mathbf{H}_{S,R}$ and $\mathbf{H}_{S,D}$, respectively. The relay node then performs the SM demodulation [18] for antenna index $a_S(\tau_1)$ and modulated signal $c_S(\tau_1)$.

In time slot 2, the demodulated sequence $\tilde{\mathbf{c}}_1$ is given into the RS_1 decoder to generate the estimated information sequence $\mathbf{m}_1$. The sequence $\mathbf{m}_2$ is then selected from $\mathbf{m}_1$ and again encoded by the RS code $RS_2(N, K_2)$ of dimension K_2 and length N over GF(2^n). The RS code RS_2 has the minimum distance $d_2 = N - K_2 + 1$. After the encoding of RS code RS_2, the generated non-binary systematic codeword $\mathbf{c}_2 = [\mathbf{p}_2, \mathbf{m}_2]$ is sent to the SM mapper that provides the transmission vector $\mathbf{x}_R(\tau_2) = [\cdots, 0, c_R(\tau_2), 0, \cdots]^T$ with $\tau_2 \in \{0, 1, \cdots, N-1\}$, where the modulated symbol $c_R(\tau_2)$ is conveyed at the $a_R(\tau_2)$th antenna. The received signal $\mathbf{y}_{R,D}(\tau_2)$ at the destination node is mathematically modeled as

$$\begin{aligned}\mathbf{y}_{R,D}(\tau_2) &= \mathbf{H}_{R,D}\mathbf{x}_R(\tau_2) + \mathbf{n}_{R,D}(\tau_2)\\ &= \mathbf{h}_{R,D}^{a_R(\tau_2)} c_R(\tau_2) + \mathbf{n}_{R,D}(\tau_2)\end{aligned} \tag{5}$$

where the definitions of $\mathbf{H}_{R,D}$ and $\mathbf{n}_{R,D}(\tau_2)$ are similar to $\mathbf{H}_{S,R}$ and $\mathbf{n}_{S,R}(\tau_1)$ in (3), respectively. $\mathbf{h}_{R,D}^{a_R(\tau_2)}$ denotes the $a_R(\tau_2)$th column of the channel matrix $\mathbf{H}_{R,D}$. Afterward, the spatial demodulation is utilized to detect the received sequences during their respective time slots. Finally, the joint decoding is performed to generate the estimated information sequence $\bar{\mathbf{m}}_1$ of $\mathbf{m}_1$ transmitted at the source node.

As mentioned earlier, the generated codeword belongs to the subcode of C of $\bar{C}$. It should be noted that the codeword with weight d_1 is likely to occur. This is due to the worst scenario that zero weight codeword is generated at the relay when the codeword with weight d_1 is produced at the source node. Therefore, the design criterion of an optimized subcode is to avoid large number of worst scenarios, which implies $\mathbf{m}_2$ must be suitably selected from $\mathbf{m}_1$ at the relay. The detailed optimized subcode design approaches by properly selecting information at the relay are given in Sect. 4.

4 Methods

In this section, two design approaches for optimizing the proposed DRSC-SM scheme are proposed, which makes the destination node generate an optimized code with a better weight distribution.

4.1 Two jointly optimized design approaches for DRSC-SM scheme

In the proposed DRSC-SM scheme, each selection in relay yields the subcode C of code $\bar{C}$. Therefore, a proper symbol selection at the relay is very pivotal in order to obtain an optimized subcode at the destination. The complexity analysis of the two optimized approaches is also presented in this section.

4.1.1 Approach 1: brute-force search over all candidates

An efficient Approach 1 for constructing an optimized subcode is proposed in this subsection. In this approach, we perform the brute-force search over all candidates (i.e., all selection patterns) at the relay to find an optimized pattern by which K_2 information symbols are selected from the decoded K_1 source information symbols. During the search, all information symbol sequences that may generate the codeword of weight $\mathrm{wt}(\mathbf{c}_1) = d_1$ at the source are considered. In order to construct an optimized code with better weight distribution at the destination, three scenarios are considered. The considered event in the first scenario contains those codewords with low weight d_1 in destination, which are jointly built by the codeword of minimum weight $\mathrm{wt}(\mathbf{c}_1) = d_1$ at the source and the codeword with weight $\mathrm{wt}(\mathbf{c}_2) = 0$ at the relay. In the second scenario, the destination node includes all codewords of low weight $d_1 + d_2$, where the codewords of minimum weights d_1 and d_2 are generated at the source and relay, respectively. The third scenario considers those codewords having low weight greater than $d_1 + d_2$ for $\mathrm{wt}(\mathbf{c}_1) = d_1$ at the source and $\mathrm{wt}(\mathbf{c}_2) > d_2$ at the relay. Assume that J_1, J_2 and J_3 represent the number of occurrences for the first, second and third scenarios, respectively. The design steps of Approach 1 are given as follows:

(1) Determine $\Omega = \{\mathbf{e}_q\}, (q = 1, 2, \cdots, K_b)$ that is the set of all information symbol sequences generating the codewords of weight $\mathrm{wt}(\mathbf{c}_1) = d_1$ at the source, where K_b denotes the number of codewords associated with weight d_1 [10].
(2) Determine the set of information selection patterns $A = \{\boldsymbol{\eta}_g\}$ with $\boldsymbol{\eta}_g = [\eta_0, \eta_1, \cdots, \eta_{K_2-1}]$ and $g = 1, 2, \cdots, \Phi$, where $\eta_l \in \{1, 2, \cdots, K_1\}$ for $l = 0, 1, \cdots, K_2 - 1$ denotes the position of the selected symbols in the K_1 symbols, and Φ is expressed as

$$\Phi = \binom{K_1}{K_2} = \frac{K_1!}{K_2!(K_1 - K_2)!} \tag{6}$$

(3) For the first worst scenario, find out J_1 for all $\mathbf{e}_q \in \Omega$ by keeping each information selection pattern $\boldsymbol{\eta}_g \in A$ fixed at the relay.
(4) Pick up selection patterns $\boldsymbol{\eta}_g$ resulting in the minimum value of J_1, i.e., min(J_1) and store them in the set B. If B has cardinality $|B| = 1$, go to step 9 else move to next step.
(5) For the second worst scenario, find out J_2 for all $\mathbf{e}_q \in \Omega$ by keeping each information selection pattern $\boldsymbol{\eta}_g \in B$ fixed at the relay.
(6) Pick up selection patterns $\boldsymbol{\eta}_g$ that result in min(J_2) and store them in the set C. If $|C| = 1$, go to step 9 else move to next step.
(7) For the third worst scenario, find out J_3 for all $\mathbf{e}_q \in \Omega$ by keeping each information selection pattern $\boldsymbol{\eta}_g \in C$ fixed at the relay.
(8) Pick up selection patterns $\boldsymbol{\eta}_g$ that result in min(J_3) and store them in the set E. If $|E| = 1$, go to step 9. If not, E is used as the update of the set C, increase the codeword weight $\mathrm{wt}(\mathbf{c}_2)$ by 1 at the relay, and then go back to step 7.
(9) Pick up the unique information selection pattern $\boldsymbol{\eta}^{(1)} = \boldsymbol{\eta}_g$ and finish Approach 1.

4.1.2 Approach 2: local search over partial candidates

As presented in Sect. 4.1.1, Approach 1 can effectively choose the optimized selection pattern from the total Φ selection patterns, during which all the information symbol sequences generating the codewords with weight $\mathrm{wt}(\mathbf{c}_1) = d_1$ at the source are considered. Therefore, for the larger block length code, the search complexity of Approach 1 is relatively high. To low the computational complexity of Approach 1, we propose the local search Approach 2. Different from Approach 1, Approach 2 searches for the optimized selection pattern from the partial candidates of the total Φ selection patterns, during which we only consider the partial information symbol sequences resulting in the codeword weight $\mathrm{wt}(\mathbf{c}_1) = d_1$ at the source. The following steps show the search process:

(1) Determine the set Ω' of partial information symbol sequences resulting in the codeword weight $\mathrm{wt}(\mathbf{c}_1) = d_1$ at the source. Since the source information sequence $\mathbf{e}_q$ generating $\mathrm{wt}(\mathbf{c}_1) = d_1$ can be searched from those information sequences of weight $0 < \mathrm{wt}(\mathbf{e}_q) \le d_1$, it implies that $\mathbf{e}_q$ has at least $\mu = K_1 - \min(K_1, d_1)$ zeros. The set Ω' can be obtained by the following method:

   (i) Divide the information sequence $\mathbf{e}_q$ of length K_1 into two parts. Scenario (a): the first $\lceil K_1/2 \rceil$ symbols form the first part and the remaining $K_1 - \lceil K_1/2 \rceil$ symbols form the last part, where $\lceil \cdot \rceil$ denotes ceil operation. Scenario (b): the first $K_1 - \lceil K_1/2 \rceil$ symbols constitute the first part and the remaining $\lceil K_1/2 \rceil$ symbols constitute the last part. The symbol distribution of the information sequence $\mathbf{e}_q$ is shown in Fig. 3.
   (ii) Determine the positions of μ zeros in the information sequence $\mathbf{e}_q$. Scenario (a): the i $(\lceil \mu/2 \rceil \le i \le \min(\mu, \lceil K_1/2 \rceil))$ zeros are randomly distributed in the first part of Fig. 3a and other $\mu - i$ zeros are uniquely assigned in the second

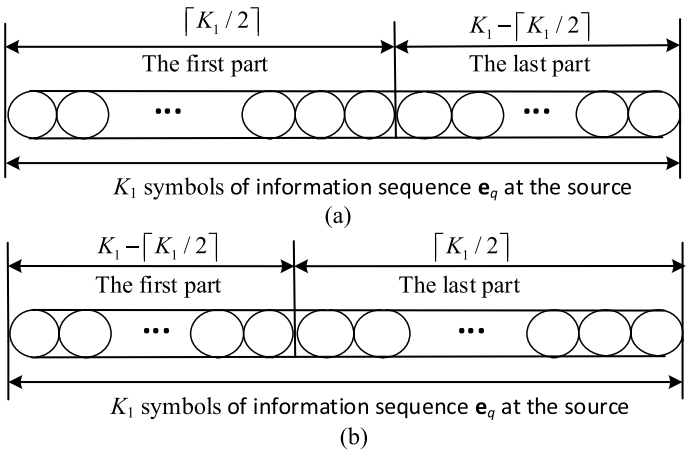

Fig. 3 Information sequence with more symbols in **a** first part, **b** last part. For information sequence with length K_1 at the source node, its symbols are divided into two cases. One case is the first part has more symbols, and the other case is the last part has more symbols. **a** denotes the symbol distribution diagram of information sequence with more symbols in the first part. **b** denotes the symbol distribution diagram of information sequence with more symbols in the last part

part of Fig. 3a. Scenario (b): the i zeros are randomly distributed in the last part of Fig. 3b and the other $\mu - i$ zeros are uniquely assigned in the first part of Fig. 3b.

(iii) Based on the above two substeps, we get the information symbol sequence set $\Omega' = \{\mathbf{e}'_{\bar{q}}\}$ with $\bar{q} = 1, 2, \cdots, |\Omega'|$, where Ω' is the subset of Ω.

(2) Determine the set $A^{'}$ of partial selection patterns.

(i) Select K_2 symbols out of K_1 source message symbols. Scenario (a): randomly select t ($\lceil K_2/2 \rceil \leq t \leq \min(K_2, \lceil K_1/2 \rceil)$) symbols from the first part of Fig. 3a, and the other $K_2 - t$ symbols are uniquely selected from the remaining part of Fig. 3a. Scenario (b): randomly select t symbols from the last part of Fig. 3b, and the other $K_2 - t$ symbols are uniquely selected from the first part of Fig. 3b.

(ii) Based on the positions of the selected K_2 symbols in the above substep, we get the set $A^{'} = \{\boldsymbol{\eta}^{'}_{\bar{g}}\}$ of selection patterns $\boldsymbol{\eta}'_{\bar{g}} = [\eta'_0, \eta'_1, \cdots, \eta'_{K_2-1}]$, where $\bar{g} = 1, 2, \cdots, |A'|$ and $A^{'}$ is the subset of A.

(3) The other steps follow steps 3–9 of the brute-force search method. Lastly, pick up this unique selected pattern $\boldsymbol{\eta}^{(2)} = \boldsymbol{\eta}^{'}_{\bar{g}}$ and finish Approach 2.

The determined $\boldsymbol{\eta}^{(2)}$ is fixed in the relay and K_2 symbols are selected from K_1 source information symbols for further encoding by the RS code $RS_2(N, K_2)$. At the destination, an optimized code with a better weight distribution is generated.

4.1.3 Design example for two approaches

In order to better understand the above two approaches, a simple example is listed here. In our example, we consider the distributed RS codes employing $RS_1(N, K_1) = RS_1(15, 13)$

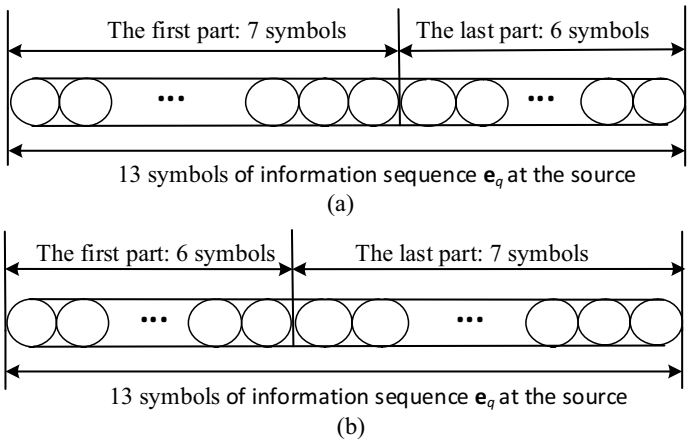

Fig. 4 Information sequence with 7 symbols in **a** first part, **b** last part. For information sequence with length $K_1 = 13$ at the source node, its symbols are divided into two cases. One case is the first part has more symbols (7 symbols), and the other case is that the last part has more symbols (7 symbols). **a** denotes the symbol diagram of information sequence with more symbols (7 symbols) in the first part. **b** denotes the symbol diagram of information sequence with more symbols (7 symbols) in the last part

Table 3 Five information selection patterns from 1716 patterns that result in min(J_1) and min(J_2)

No.	Selection patterns (η_g)	J_1	J_2
1	[1 2 3 4 5 6 13]	840	4340
2	[1 2 3 5 8 10 12]	840	4224
3	[1 3 4 6 9 11 13]	840	4400
4	[1 3 5 8 9 11 12]	840	4140
5	[2 3 4 6 9 11 13]	840	4800

and $RS_2(N, K_2) = RS_2(15, 7)$ over GF(2^4) that is constructed using polynomial $1 + X + X^4$, where $RS_1(15, 13)$ and $RS_2(15, 7)$ are placed at the source and relay nodes, respectively. At the relay, only $K_2 = 7$ symbols are selected out of $K_1 = 13$ recovered symbols. First, Approach 1 is used to determine the selection pattern at the relay as follows:

(1) Determine the set $\Omega = \{\mathbf{e}_q\}$ of information sequences generating the codeword of weigh three for $RS_1(15, 13)$ at the source, where $|\Omega| = 6825$ with the help of computer simulations or theoretical analysis in [19].
(2) Determine the set $A = \{\boldsymbol{\eta}_g\}$ that consists of all information selection patterns, i.e., 1716 patterns $\boldsymbol{\eta}_g = [\eta_0, \eta_1, \cdots, \eta_6]$.
(3) Determine the parameter J_1 of the first worst scenario by keeping each $\boldsymbol{\eta}_g \in A$ fixed at the relay and transmitting all $\mathbf{e}_q \in \Omega$, and find out $\min(J_1) = 840$.
(4) Select the patterns $\boldsymbol{\eta}_g$ resulting in $\min(J_1) = 840$ and store them in B. Since $|B| = 1716 > 1$, then we proceed to the next step. Table 3 presents five patterns out of 1716 patterns causing $\min(J_1) = 840$.
(5) Determine the parameter J_2 of the second worst scenario by keeping each $\boldsymbol{\eta}_g \in B$ fixed at the relay and transmitting all $\mathbf{e}_q \in \Omega$, and find out $\min(J_2) = 4140$, also presented in Table 3.

(6) Select the patterns $\boldsymbol{\eta}_g$ resulting in $\min(J_2) = 4140$ and store them in C. Now, $|C| = 1$; therefore, we move to step 9 and terminate Approach 1. Then, the unique selection pattern is defined such as $\boldsymbol{\eta}^{(1)} = \boldsymbol{\eta}_g = [1, 3, 5, 8, 9, 11, 12]$.

Now, we employ Approach 2 to determine the selection pattern at the relay. Since the minimum weight of codewords generated by RS_1 (15,13) is three, the corresponding information sequences of length thirteen have at least ten zeros. The detailed process that obtains the selection pattern is presented as follows:

(1) Determine the positions of ten zeros of information sequence at the source. Scenario (a): the $i \quad (5 \leq i \leq 7)$ zeros 10 zeros are randomly distributed in the first part (7 symbols) of Fig. 4a and the other $10 - i$ zeros are uniquely assigned in the remaining part (6 symbols) of Fig. 4a. Scenario (b): the i zeros of 10 zeros are randomly distributed in the last part (7 symbols) of Fig. 4b and the other $10 - i$ zeros are uniquely assigned in the remaining part (6 symbols) of Fig. 4b. According to this way, we obtain the set $\Omega' = \{\mathbf{e}'_{\bar{q}}\}$ with $|\Omega'| = 1965$, which includes partial information sequences generating codewords of weight three.
(2) 7 symbols are selected from 13 symbols. Scenario (a): randomly select $t \quad (4 \leq t \leq 7)$ symbols from the first 7 symbols of Fig. 4a but other $7 - t$ symbols are uniquely selected from other 6 symbols of Fig 4a. Scenario (b): randomly select t symbols from the last 7 symbols of Fig. 4b but other $7 - t$ symbols are uniquely selected from those remaining 6 symbols of Fig. 4b. Based on this method, we determine the set $A' = \{\boldsymbol{\eta}'_{\bar{g}}\}$ of information selection patterns $\boldsymbol{\eta}'_{\bar{g}} = [\eta'_0, \eta'_1, \cdots, \eta'_6]$ and find out $|A'| = 128$.
(3) Determine the parameter J_1 of the first worst scenario by keeping each $\boldsymbol{\eta}'_{\bar{g}} \in A'$ fixed at the relay and transmitting all $\mathbf{e}'_{\bar{q}} \in \Omega'$, and find out $\min(J_1) = 195$.
(4) Select the patterns $\boldsymbol{\eta}'_{\bar{g}}$ resulting in $\min(J_1) = 195$ and store them in B'. Since $|B'| = 128 > 1$, then we proceed to the next step. Table 4 presents five patterns out of 128 patterns causing $\min(J_1) = 195$.
(5) Determine the parameter J_2 of the second worst scenario by keeping each $\boldsymbol{\eta}'_{\bar{g}} \in B'$ fixed at the relay and transmitting all $\mathbf{e}'_{\bar{q}} \in \Omega'$, and find out $\min(J_2)$=68, also presented in Table 4.
(6) Select the patterns $\boldsymbol{\eta}'_{\bar{g}}$ resulting in $\min(J_2)$=68 and store them in C'. Now $|C'| = 1$; therefore, we move to step 9 and terminate Approach 2. Accordingly, the selection pattern is chosen as $\boldsymbol{\eta}^{(2)} = \boldsymbol{\eta}'_{\bar{g}} = [3, 5, 7, 9, 10, 11, 12]$.

Table 4 Five information selection patterns from 128 patterns that result in $\min(J_1)$ and $\min(J_2)$

No.	Selection patterns ($\boldsymbol{\eta}'_{\bar{g}}$)	J_1	J_2
1	[1 2 3 4 6 11 13]	195	100
2	[2 3 4 8 10 11 12]	195	86
3	[1 2 3 5 6 8 9]	195	89
4	[3 5 7 9 10 11 12]	195	68
5	[3 6 7 8 9 10 12]	195	88

4.1.4 Complexity analysis

The complexity of both proposed design approaches is compared in terms of multiplication and addition operations in this subsection. At the source, encoding one information sequence with length K_1 requires $\varpi_S^{\times} = K_1(N-K_1)$ multiplication operations and $\varpi_S^{+} = K_1(N-K_1)$ addition operations. Therefore, the total $\varpi_S = \varpi_S^{\times} + \varpi_S^{+} = 2K_1(N-K_1)$ elementary operations are involved in encoding one information sequence. Similarly, encoding one information sequence with length K_2 at the relay requires the total $\varpi_R = \varpi_R^{\times} + \varpi_R^{+} = 2K_2(N-K_2)$ elementary operations, where $\varpi_R^{\times} = K_2(N-K_2)$ and $\varpi_R^{+} = K_2(N-K_2)$.

In Approach 1, $|\Omega|$ information sequences generating the codewords with $\mathrm{wt}(\mathbf{c}_1) = d_1$ at the source are considered. Thus, the total number of elementary operations at the source is $\varpi_{S,\Omega} = |\Omega|\varpi_S = 2K_1|\Omega|(N-K_1)$. At the relay, the K_2 symbols are selected from the decoded K_1 source symbols for further encoding, and therefore, encoding $|\Omega|$ information blocks needs to perform $\varpi_{R,\Omega} = 2K_2|\Omega|(N-K_2)$ for each selection pattern. Let the number of considered selection patterns be $M_{d_1}^{(1)}$, $M_{d_1+d_2}^{(1)}$, $M_{d_1+d_2+1}^{(1)}$,..., $M_{2N}^{(1)}$, respectively, when finding out the number of codeword weight d_1, d_1+d_2, d_1+d_2+1,..., $2N$ at the destination. If the optimized selection pattern $\boldsymbol{\eta}^{(1)}$ is determined in finding out the number of codeword weight w at the destination, the computational complexity of Approach 1 is then expressed as

$$\varpi_{\text{Approach1}} = \varpi_{S,\Omega} + \varpi_{R,\Omega}\left(M_{d_1}^{(1)} + M_{d_1+d_2}^{(1)} + M_{d_1+d_2+1}^{(1)} + \ldots + M_{w}^{(1)}\right) \tag{7}$$

In Approach 2, we consider $|\Omega'|$ information sequences resulting in the codewords with $\mathrm{wt}(\mathbf{c}_1) = d_1$ in the source, and the overall elementary operation number is then denoted as $\varpi_{S,\Omega'} = |\Omega'|\varpi_S = 2K_1|\Omega'|(N-K_1)$. Then, for each selection pattern, encoding $|\Omega'|$ information sequences at the relay requires $\varpi_{R,\Omega'} = |\Omega'|\varpi_R = 2K_2|\Omega'|(N-K_2)$ elementary operations. If the optimized selection pattern $\boldsymbol{\eta}^{(2)}$ is determined in finding out the number of codeword weight w' at the destination, the complexity of Approach 2 is represented as

$$\varpi_{\text{Approach2}} = \varpi_{S,\Omega'} + \varpi_{R,\Omega'}\left(M_{d_1}^{(2)} + M_{d_1+d_2}^{(2)} + M_{d_1+d_2+1}^{(2)} + \ldots + M_{w'}^{(2)}\right) \tag{8}$$

where $M_{d_1}^{(2)}$, $M_{d_1+d_2}^{(2)}$, $M_{d_1+d_2+1}^{(2)}$,..., $M_{w'}^{(2)}$ are the number of considered selection patterns, respectively, in finding out the number of codeword weight d_1, d_1+d_2, d_1+d_2+1 ,..., w' at the destination. Based on Eqs. (7) and (8), we can get the complexity of Approach 1 and Approach 2. As presented in Sect. 4.1.3, the parameters $|\Omega'| = 1965$, $M_{d_1}^{(2)} = |A'| = 128$ and $M_{d_1+d_2}^{(2)} = |B'| = 128$ in Approach 2 are less than the parameters $|\Omega| = 6825$, $M_{d_1}^{(1)} = |A| = 1716$ and $M_{d_1+d_2}^{(1)} = |B| = 1716$ in Approach 1, respectively. Thus, Approach 2 has a reduced complexity over Approach 1.

4.2 Error performance comparisons of two approaches

We present the BER performance curves of ideal DRSC-SM scheme ($\lambda_{S,R} = \infty$) with RS_1 (15,13) and RS_2 (15,7) based on two design approaches as presented in Fig. 5. In the simulation, the smart decoding algorithm discussed in Sect. 5, 4-QAM and $N_\mathrm{t} = N_\mathrm{r} = 4$ are used. Through the simulated results, we notice that the DRSC-SM

Table 5 Relationship between different distributed RS codes and optimized selection patterns

No.	Distributed RS codes		Optimized selection patterns	
	$RS_1(N, K_1)$	$RS_2(N, K_2)$	$\eta^{(1)}$	$\eta^{(2)}$
1	$RS_1(15, 13)$	$RS_2(15, 7)$	[1 3 5 8 9	[3 11 5 12] 9 10 11 12]
2	$RS_1(31, 25)$	$RS_2(31, 13)$	–	[2 3 4 6 8 9 10 13 15 16 17 19 22]
3	$RS_1(63, 61)$	$RS_2(63, 41)$	–	[1 2 4 5 6 7 9 10 12 13 14 16 17 19 21 23 24 25 27 29 30 32 33 35 37 38 39 41 42 43 46 47 49 51 52 54 57 58 59 60 61]

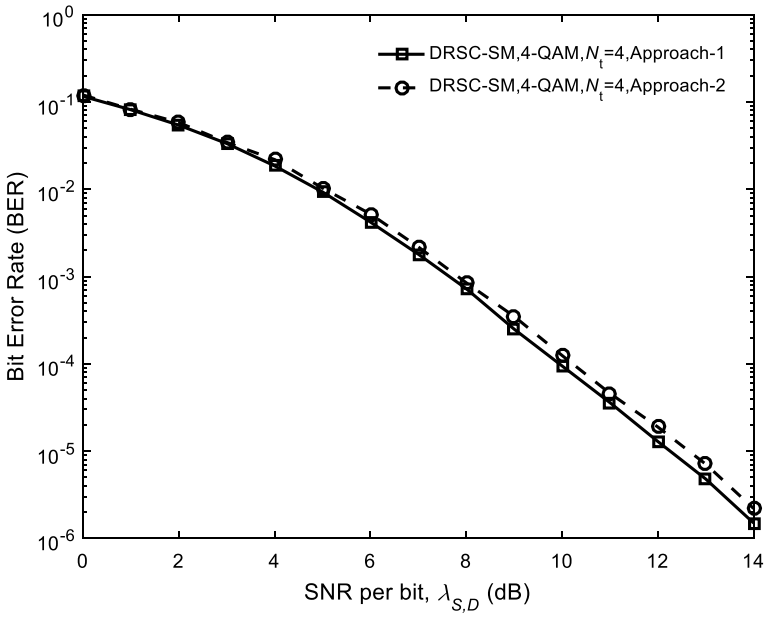

Fig. 5 Performance of DRSC-SM scheme (4-QAM) with $RS_1(15, 13)$ and $RS_2(15, 7)$ employing Approach 1 and Approach 2. The dashed line with circle mark denotes the BER performance of DRSC-SM scheme under Approach 2, and the solid line with square mark denotes the BER performance of DRSC-SM scheme under Approach 1

scheme under Approach 1 and Approach 2 perform nearly identical performance at low signal-to-noise ratio (SNR). Moreover, at high SNR, the DRSC-SM scheme employing Approach 2 is only 0.15 dB worse than that of Approach 1 at BER $\approx 2.2 \times 10^{-6}$. This phenomenon reveals the validity of our proposed Approach 2 performing partial search as compared to Approach 1 performing brute-force search. Similarly, we investigate the other distributed RS-coded SM schemes in this paper, whose distributed RS codes and the corresponding optimized selection patterns are presented in Table 5.

In Sect. 4.1.2, the general description of Approach 2 has been presented. Based on substep (i) in step 2, multiple reasonable selections of K_2 information symbols from the K_1 information symbols at the relay can be obtained. If we apply the selection way to the selection process of t symbols from $\lceil K_1/2 \rceil$ symbols in scenarios (a) and (b) of substep (i) in step 2, Approach 2 will be further modified into an approach with lower complexity. In Sect. 6, we will analyze the system performance under the modified Approach 2.

It should be noted that our presented search approaches determining the optimized selection pattern are the general approaches, where the selection can be binary bit selection or non-binary symbol selection. In our paper, we have already applied these methods to the symbol selection of RS codes which are non-binary.

5 Joint RS decoding of DRSC-SM scheme

Joint decoding at the destination is one of the key features of coded cooperative systems. In this section, three decoding algorithms, i.e., naive algorithm, smart algorithm and improved smart algorithm, are presented to jointly decode the transmitted sequences.

5.1 Naive decoding algorithm

In this subsection, the naive decoding algorithm is presented as follows:

(1) Give the first and second parts of demodulated $|\hat{\mathbf{c}}_1|\hat{\mathbf{c}}_2|$ into the RS_1 decoder and RS_2 decoder, respectively. The Euclidean algorithm [19] which is based on the greatest common divisor (GCD) is employed in the M-ary $RS_k (k = 1, 2)$ decoder. Then, the estimated non-binary information sequences $\hat{\mathbf{m}}_1$ and $\hat{\mathbf{m}}_2$ are obtained.
(2) Select a threshold value δ, which is taken as the SNR where the BER performance (individual performance) of RS_1 and RS_2 codes crosses each other or meets each other.
(3) If SNR$< \delta$, then the estimated sequence of $\mathbf{m}_1$ is taken as $\bar{\mathbf{m}}_1 = \hat{\mathbf{m}}_1$. If SNR$\geq \delta$, those selected K_2 symbols of sequence $\hat{\mathbf{m}}_1$ are replaced with sequence $\hat{\mathbf{m}}_2$, then the new generated sequence $\bar{\mathbf{m}}_1$ of $\hat{\mathbf{m}}_1$ is eventually viewed as the estimated sequence of $\mathbf{m}_1$.

In channel coding, the BER performance of code with more error correcting capability is worse than the code with less error correcting capability for low SNR regime, while it outperforms the less error correcting capability code over high SNR regime. Thus, because of large d_2 of RS code RS_2, for high SNR all K_2 symbols of $\hat{\mathbf{m}}_2$ are more reliable than those selected K_2 symbols of $\hat{\mathbf{m}}_1$, but vice versa for low SNR. This is the reason for applying the judgment criteria in step 3.

5.2 Smart decoding algorithm

We use the naive decoding algorithm as a benchmark and propose another decoding algorithm, i.e., smart decoding algorithm. The steps of the smart decoding algorithm are shown as follows:

(1) Firstly feed the second part $\hat{\mathbf{c}}_2$ of demodulated $|\hat{\mathbf{c}}_1|\hat{\mathbf{c}}_2|$ into the RS_2 decoder, which generates the estimated systematic non-binary information symbol sequence $\hat{\mathbf{m}}_2$.
(2) Replace those selected K_2 symbols of the sequence $\hat{\mathbf{c}}_1 = [\hat{\mathbf{p}}_1, \hat{\mathbf{m}}_1']$ comprised of the parity symbol sequence $\hat{\mathbf{p}}_1$ and information symbol sequence $\hat{\mathbf{m}}_1'$ by using the sequence $\hat{\mathbf{m}}_2$. The joint source relay sequence $\bar{\mathbf{c}}_1 = [\hat{\mathbf{p}}_1, \hat{\mathbf{m}}_1'']$ of length N is then produced.
(3) Send the generated joint source relay sequence $\bar{\mathbf{c}}_1$ to the RS_1 decoder. Then, we obtain an estimate $\bar{\mathbf{m}}_1$ of information symbol sequence $\mathbf{m}_1$.

5.3 Improved smart decoding algorithm

In this subsection, we propose a new decoding algorithm, i.e., the improved smart decoding algorithm. The decoding process is realized by the following steps:

(1) The RS_2 decoder receives the second part $\hat{\mathbf{c}}_2$ of the demodulated sequence $|\hat{\mathbf{c}}_1|\hat{\mathbf{c}}_2|$ to yield the estimation $\hat{\mathbf{m}}_2$ of the information symbol sequence $\mathbf{m}_2$ of the RS_2 encoder.
(2) The estimated information symbol sequence $\hat{\mathbf{m}}_2$ and the first part $\hat{\mathbf{c}}_1 = [\hat{\mathbf{p}}_1, \hat{\mathbf{m}}_1']$ of $|\hat{\mathbf{c}}_1|\hat{\mathbf{c}}_2|$ are given into the decision combiner block.
(3) Choose a threshold value δ that is the SNR where the error performance of the codes RS_1 and RS_2 meets each other. Since the minimum distance of the RS_2 code is larger than that of the RS_1 code, the RS_2 code has a better error correcting capability. Based on the channel coding theory [19], the RS_1 code performs better performance than the RS_2 code for SNR$< \delta$, but the latter outperforms the former for SNR$\geq \delta$.
(4) If SNR$< \delta$, the decision combiner directly uses the sequence $\hat{\mathbf{c}}_1$ as the output $\bar{\mathbf{c}}_1$, i.e., $\bar{\mathbf{c}}_1 = \hat{\mathbf{c}}_1$.
(5) If SNR$\geq \delta$, $\hat{\mathbf{m}}_2$ is more reliable than the K_2 symbols (placed in the selected K_2 positions) in $\hat{\mathbf{m}}_1'$. Thus, we replace the selected K_2 symbols of $\hat{\mathbf{m}}_1'$ by using the estimated information symbol sequence $\hat{\mathbf{m}}_2$, i.e., the output of the decision combiner is $\bar{\mathbf{c}}_1 = [\hat{\mathbf{p}}_1, \hat{\mathbf{m}}_1'']$.
(6) Finally, the RS_1 decoder accepts the sequence $\bar{\mathbf{c}}_1$ from the decision combiner and generates the estimation $\bar{\mathbf{m}}_1$ of the source information symbol sequence $\mathbf{m}_1$.

The improved smart algorithm cleverly incorporates the idea of threshold selection, and flexibly selects more reliable symbols to enter the RS_1 decoder according to the change of SNR. However, the smart algorithm directly uses the decoded K_2 symbols of the RS_2 decoder as the input of the RS_1 decoder over the whole SNR. Therefore, the proposed improved smart algorithm can effectively ameliorate the performance of the smart algorithm under low SNR, as presented in Sect. 6.

6 Results and discussion

The BER performance of DRSC-SM scheme and reference schemes through quasi-static Rayleigh fading channel is presented in this section. Three cases of distrusted RS codes presented in Table 5 are mainly considered to generalize our proposed DRSC-SM scheme. For the first case, we employ the RS codes over GF(2^4) constructed based on the polynomial $1 + X + X^4$. Furthermore, the RS codes over GF(2^5) and GF(2^6) which are constructed using polynomials $1 + X^2 + X^5$ and $1 + X + X^6$ are considered in the second and third cases, respectively. The modulation schemes such as 4-QAM, 8-QAM and 16-QAM are applied in the first, second and third cases, respectively. The SNR per bit between the $S - D$ link is represented as $\lambda_{S,D}$. Similarly, $\lambda_{S,R}$ and $\lambda_{R,D}$ denote the SNR per bit for the $S - R$ and $R - D$ links, respectively. It is assumed that the relay node has a 2 dB SNR gain over the source node, i.e., $\lambda_{R,D} = \lambda_{S,D} + 2$ dB. The Euclidean decoding algorithm is used for overall simulation. Furthermore, we assume that all corresponding receivers have perfect channel state information.

6.1 BER performance of DRSC-SM scheme under different subcode design approaches

In this section, the BER performance of DRSC-SM scheme under different subcode design approaches for the first case is illustrated in Fig. 6. The ideal source-to-relay channel ($\lambda_{S,R} = \infty$), $N_t = N_r = 4$, maximum likelihood (ML) detection and joint RS decoding (smart algorithm) are used. The simulated results show the benefits of Approach 1 and Approach 2 as compared with the randomly selected approach, which is due to the fact that Approach 1 and Approach 2 effectively reduce the number of minimum weight codewords generated at the destination. The phenomenon illustrates the advantageous effect of proper symbol selection of our presented approaches on the performance of DRSC-SM scheme. In addition, Fig. 6 shows that the system performance under Approach 1 is very near to that under Approach 2 for low SNR. Also, for high SNR, the performance degradation is negligible. This is because the optimized code generated at the destination under the two search approaches have the same minimum distance (i.e., 3). Thus, this fully demonstrates the effectiveness of the local search Approach 2 over the brute-force search Approach 1. Furthermore, the system performance under ($\lambda_{S,R} = \infty$) employing the smart decoding algorithm with the randomly selected approach and Approach 2 under ML detection and $N_t = N_r = 4$ for the second and third cases is presented in Figs. 7 and 8. It is seen that the DRSC-SM scheme with Approach 2 achieves better performance than that with the randomly selected approach. It can be explained that Approach 2 generates an optimized code with a larger minimum distance (i.e., 32 for the second case and 30 for the third case) at the destination.

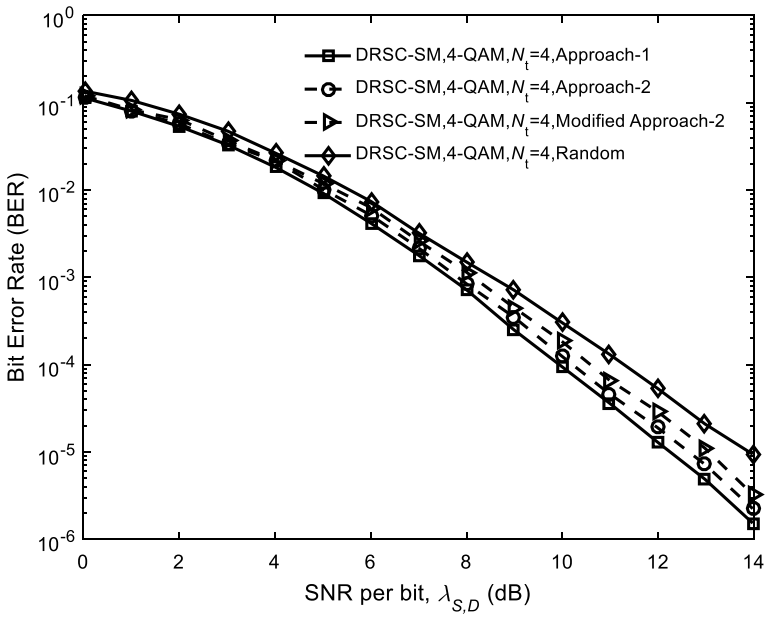

Fig. 6 Performance of DRSC-SM scheme (4-QAM) with $RS_1(15, 13)$ and $RS_2(15, 7)$ under different approaches. The solid line with diamond mark denotes the BER performance of DRSC-SM scheme under random approach. The dashed line with circle mark denotes the BER performance of DRSC-SM scheme under Approach 2. The dashed line with right triangle mark denotes the BER performance of DRSC-SM scheme under modified Approach 2. The solid line with square mark denotes the BER performance of DRSC-SM scheme under Approach 1

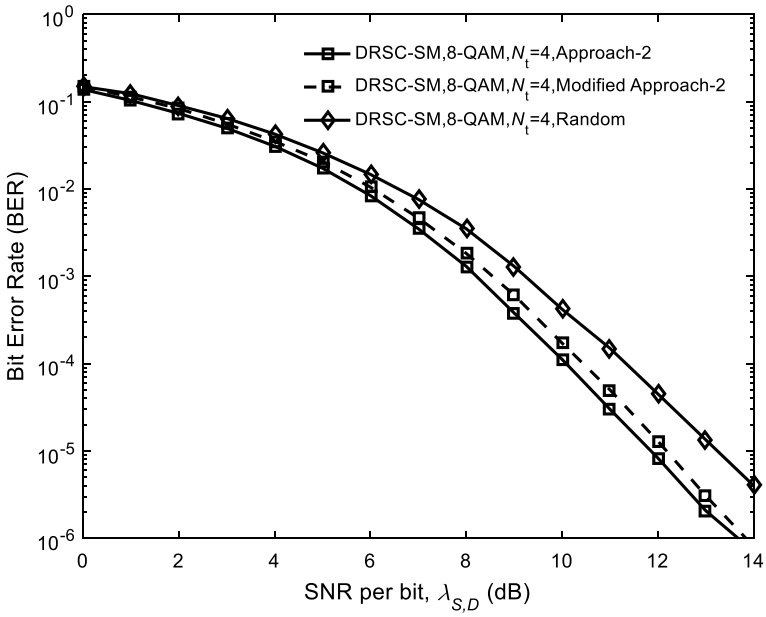

Fig. 7 Performance of DRSC-SM scheme (8-QAM) with $RS_1(31, 25)$ and $RS_2(31, 13)$ under different approaches. The solid line with diamond mark denotes the BER performance of DRSC-SM scheme under random approach. The solid line with square mark denotes the BER performance of DRSC-SM scheme under Approach 2. The dashed line with square mark denotes the BER performance of DRSC-SM scheme under modified Approach 2

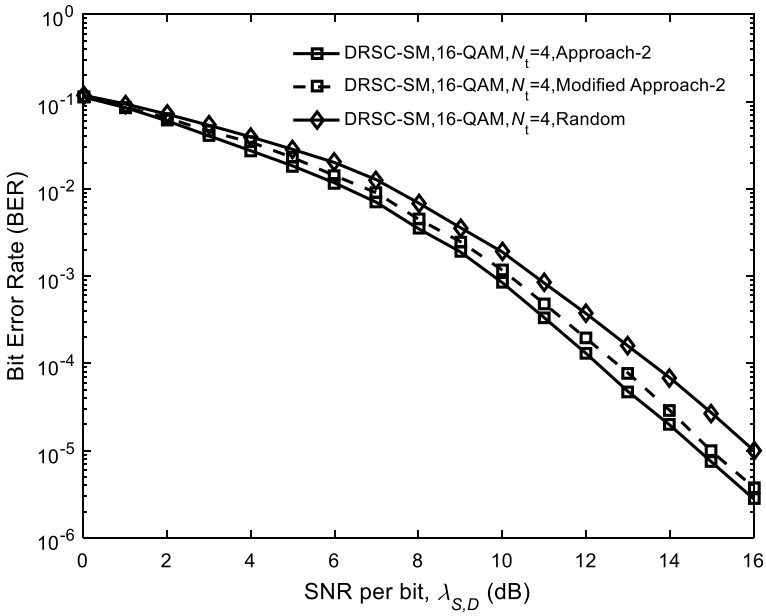

Fig. 8 Performance of DRSC-SM scheme (16-QAM) with $RS_1(63, 61)$ and $RS_2(63, 41)$ under different approaches. The solid line with diamond mark denotes the BER performance of DRSC-SM scheme under random approach. The solid line with square mark denotes the BER performance of DRSC-SM scheme under Approach 2. The dashed line with square mark denotes the BER performance of DRSC-SM scheme under modified Approach 2

Moreover, Figs. 6, 7 and 8 also show the system performance under the modified Approach 2 that has lower complexity than Approach 2. The simulation results demonstrate that the performance difference between the modified Approach 2 and Approach 2 is relatively small. For example, at SNR=14 dB in Fig. 6, the DRSC-SM scheme under Approach 2 and the modified Approach 2 achieves the approximate performances, i.e., 3.2×10^{-6} and 2.2×10^{-6}. The phenomenon reflects the rationality of the modified Approach 2 with the reduced complexity.

6.2 Performance of DRSC-SM scheme employing different decoding algorithms

The performance comparison of DRSC-SM employing joint decoding algorithms (naive algorithm, smart algorithm and improved smart algorithm) for the first case is shown in Fig. 9. The ideal source-to-relay channel condition, i.e., $\lambda_{S,R} = \infty$, ML detection and $N_t = N_r = 4$, are supposed. As shown in Fig. 9a, for SNR$\geq$ 3, the DRSC-SM system using the smart algorithm outperforms that using the naive one when the code resulted by Approach 1 is constructed at the destination. The reason behind the performance gains is that the more reliable decoded symbols of the RS_2 decoder are used as the input to the RS_1 decoder at SNR$\geq$ 3. However, in the case of SNR$<$ 3, the smart algorithm lags behind the naive algorithm. The poor performance can be ameliorated by adopting the improved smart algorithm as illustrated in Fig. 9b, which is explained that the improved smart algorithm can flexibly select more reliable symbols based on the change of SNR so that an additional advantage is given to the improved smart DRSC-SM scheme. Furthermore, Figs. 10 and 11 analyze the BER performance under different decoding algorithms for the second and third cases with $\lambda_{S,R} = \infty$, ML detection and $N_t = N_r = 4$. The simulation results confirm the effectiveness of our proposed improved smart algorithm again.

6.3 BER performance of DRSC-SM scheme over non-ideal and ideal source-to-relay channels and noncooperative scheme

Next, the BER performance of DRSC-SM over more practical scenarios ($\lambda_{S,R} \neq \infty$) and noncooperative scheme for the first, second and third cases is analyzed as shown in Figs. 12, 13 and 14, respectively. Approach 1 is applied in the first case, but Approach 2 is applied in the other two cases. Furthermore, the joint decoding (smart decoding algorithm), $N_t = N_r = 4$ and ML detection are employed in the three cases. For a fair comparison, the DRSC-SM scheme and its corresponding noncooperative scheme have an identical code rate from the destination point of view. It is noticed from Fig. 12 that the DRSC-SM scheme under $\lambda_{S,R} = \infty$ excels its noncooperative scheme under the same code rate, i.e., 13/30. At BER$= 3 \times 10^{-5}$, the DRSC-SM scheme obtains a BER performance gain of approximately 2.7 dB over the noncooperative scheme. It can be explained that the cooperation gives the performance gains to the system. Furthermore, the performance of DRSC-SM scheme under $\lambda_{S,R} = 14$ dB is near to that of DRSC-SM scheme under $\lambda_{S,R} = \infty$. However, the BER performance becomes worse when the SNR between the source S and relay R becomes poor, i.e., $\lambda_{S,R} = 8$ dB. For such a poor link, an error floor is exhibited at BER $\approx 6 \times 10^{-4}$. This is because the erroneous decoding at the relay node incurs the error propagation of destination node. The cyclic redundancy check (CRC) technique [9] can be applied to control the error propagation to some extent. However, the details are beyond the scope of this manuscript. Similarly, from Figs. 13 and

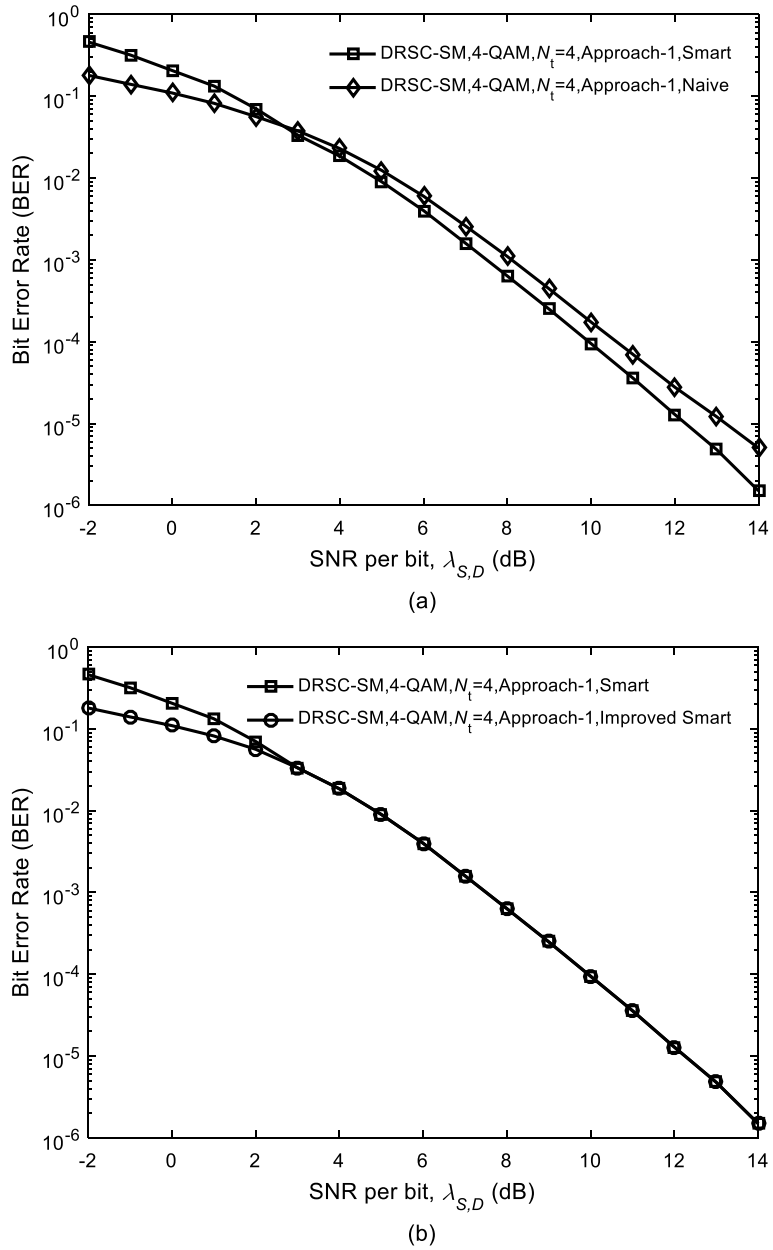

Fig. 9 Performance of DRSC-SM scheme (4-QAM) with $RS_1(15, 13)$ and $RS_2(15, 7)$ employing different algorithms. In Fig. 9a, the solid line with diamond mark denotes the BER performance of DRSC-SM scheme employing naive algorithm. The solid line with square mark denotes the BER performance of DRSC-SM scheme employing smart algorithm. In Fig. 9b, the solid line with circle mark denotes the BER performance of DRSC-SM scheme employing improved smart algorithm. The solid line with square mark denotes the BER performance of DRSC-SM scheme employing smart algorithm

14, we not only discover the superiority of ideal DRSC-SM scheme ($\lambda_{S,R} = \infty$) over non-cooperative scheme, but also observe the performance of DRSC-SM under $\lambda_{S,R} = 14$ dB and $\lambda_{S,R} = 19$ dB is near to that of ideal DRSC-SM scheme. However, when $\lambda_{S,R}$ is taken as a poor value, i.e., 9 dB and 11 dB, the BER curves of Figs. 13 and 14 will be flat at high SNR regime.

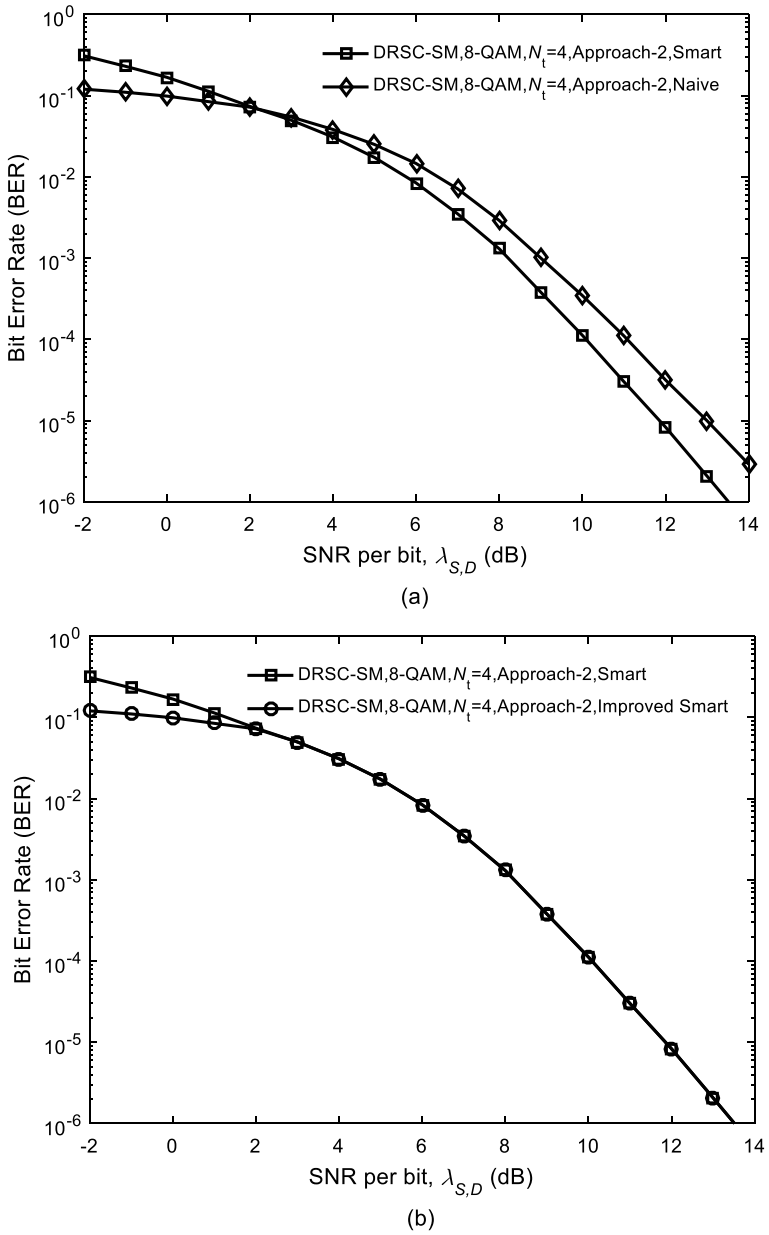

Fig. 10 Performance of DRSC-SM scheme (8-QAM) with $RS_1(31, 25)$ and $RS_2(31, 13)$ employing different algorithms. In Fig. 10a, the solid line with diamond mark denotes the BER performance of DRSC-SM scheme employing naive algorithm. The solid line with square mark denotes the BER performance of DRSC-SM scheme employing smart algorithm. In Fig. 10b, the solid line with circle mark denotes the BER performance of DRSC-SM scheme employing improved smart algorithm. The solid line with square mark denotes the BER performance of DRSC-SM scheme employing smart algorithm

6.4 BER performance of DRSC-SM scheme with various number of receive antennas

Figures 15 and 16 discuss the BER performance of DRSC-SM scheme with various number of receive antennas for the second and third cases. In Monte Carlo simulations, the joint decoding (smart algorithm), Approach 2, ML detection and $\lambda_{S,R} = \infty$ are assumed. The simulated results demonstrate that incresing N_{r} improves the performance. In Fig. 15, at SNR=10 dB, the DRSC-SM scheme with $N_{\mathrm{r}} = 2$ receiving

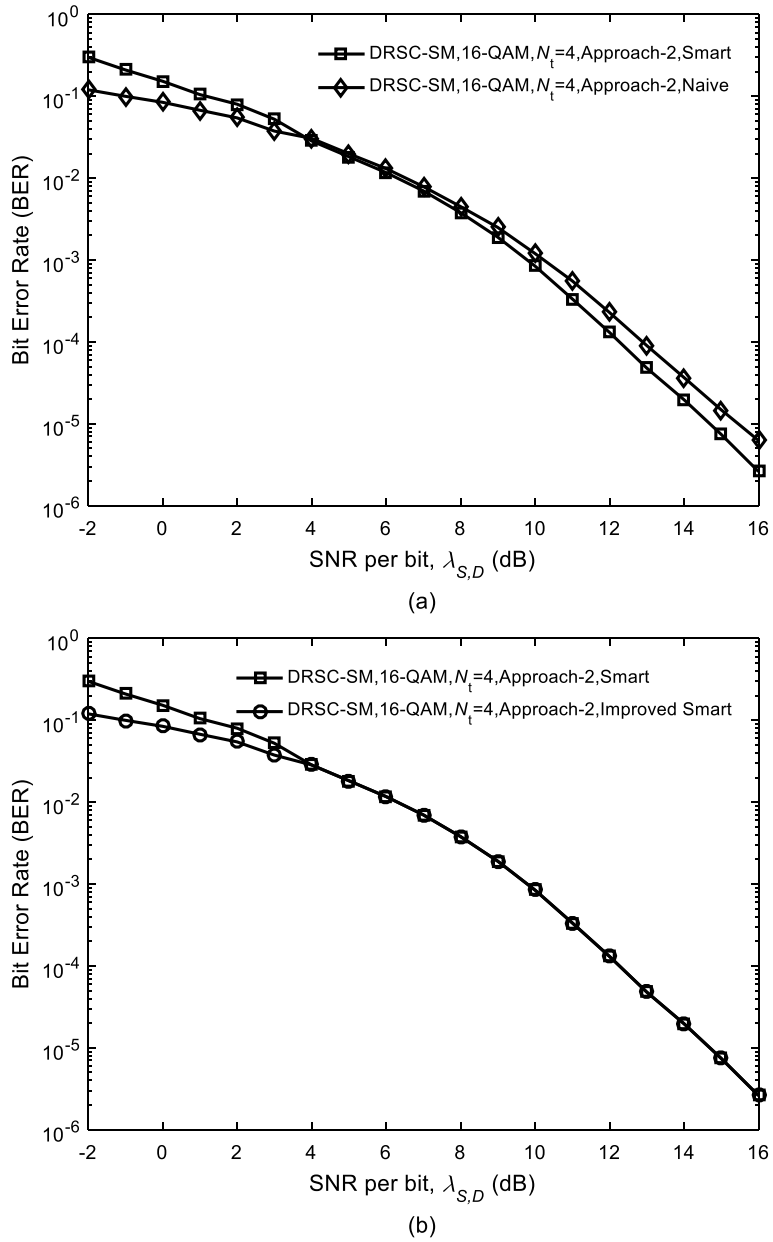

Fig. 11 Performance of DRSC-SM scheme (16-QAM) with $RS_1(63, 61)$ and $RS_2(63, 41)$ employing different algorithms. In Fig. 11a, the solid line with diamond mark denotes the BER performance of DRSC-SM scheme employing naive algorithm. The solid line with square mark denotes the BER performance of DRSC-SM scheme employing smart algorithm. In Fig. 11b, the solid line with circle mark denotes the BER performance of DRSC-SM scheme employing improved smart algorithm. The solid line with square mark denotes the BER performance of DRSC-SM scheme employing smart algorithm

antennas gets BER= 2.4×10^{-2}. When the destination uses $N_r = 3, 4$ and 6 receive antennas, the performances 1.9×10^{-3}, 1.1×10^{-4} and 2.4×10^{-7} are separately obtained at the same SNR. Furthermore, Fig. 16 presents that the DRSC-SM scheme under $N_r = 2, 3, 4$ and 6 obtains BER= $8.7 \times 10^{-3}, 6.4 \times 10^{-4}, 5 \times 10^{-5}$ and 4.1×10^{-7}, respectively, at $\lambda_{S,R} = 13$ dB. This phenomenon can be explained that augmenting its

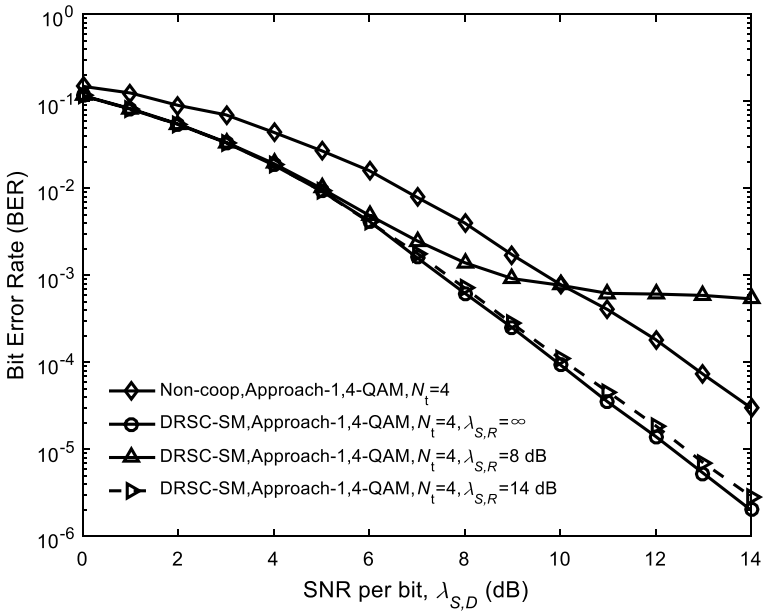

Fig. 12 Performance of DRSC-SM and noncooperative schemes (4-QAM) employing $RS_1(15, 13)$ and $RS_2(15, 7)$. The solid line with upper triangle mark demonstrates the BER performance of DRSC-SM under non-ideal source-to-relay channel ($\lambda_{S,R} = 8$ dB). The solid line with diamond mark demonstrates the BER performance of noncooperative scheme. The dashed line with right triangle mark demonstrates the BER performance of DRSC-SM under non-ideal source-to-relay channel ($\lambda_{S,R} = 14$ dB). The solid line with circle mark demonstrates the BER performance of DRSC-SM under ideal source-to-relay channel ($\lambda_{S,R} = \infty$)

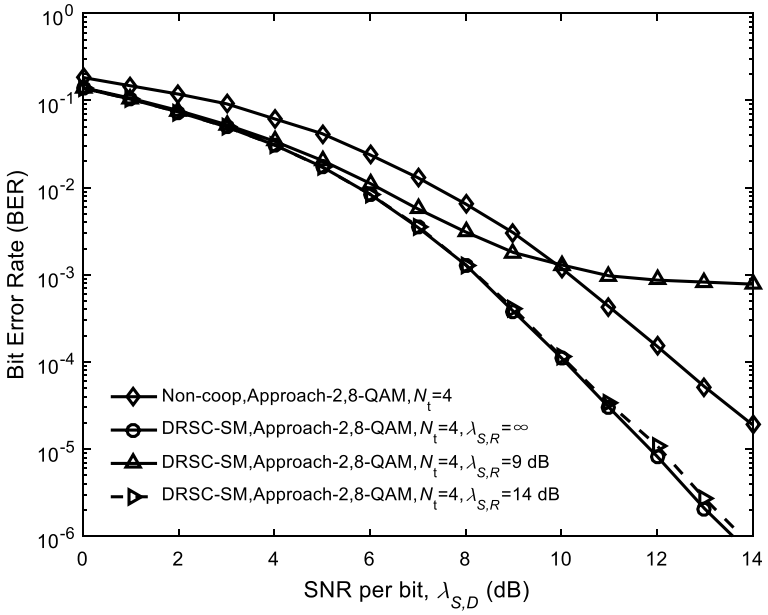

Fig. 13 Performance of DRSC-SM and noncooperative schemes (8-QAM) employing $RS_1(31, 25)$ and $RS_2(31, 13)$. The solid line with upper triangle mark demonstrates the BER performance of DRSC-SM under non-ideal source-to-relay channel ($\lambda_{S,R} = 9$ dB). The solid line with diamond mark demonstrates the BER performance of noncooperative scheme. The dashed line with right triangle mark demonstrates the BER performance of DRSC-SM under non-ideal source-to-relay channel ($\lambda_{S,R} = 14$ dB). The solid line with circle mark demonstrates the BER performance of DRSC-SM under ideal source-to-relay channel ($\lambda_{S,R} = \infty$)

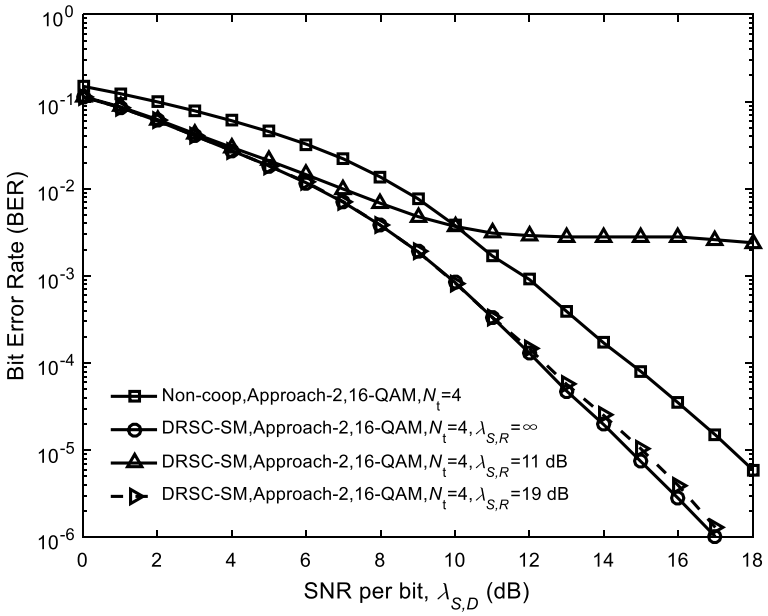

Fig. 14 Performance of DRSC-SM and noncooperative schemes (16-QAM) employing $RS_1(63, 61)$ and $RS_2(63, 41)$. The solid line with upper triangle mark demonstrates the BER performance of DRSC-SM under non-ideal source-to-relay channel ($\lambda_{S,R} = 11$dB). The solid line with square mark demonstrates the BER performance of noncooperative scheme. The dashed line with right triangle mark demonstrates the BER performance of DRSC-SM under non-ideal source-to-relay channel ($\lambda_{S,R} = 19$ dB). The solid line with circle mark demonstrates the BER performance of DRSC-SM under ideal source-to-relay channel ($\lambda_{S,R} = \infty$)

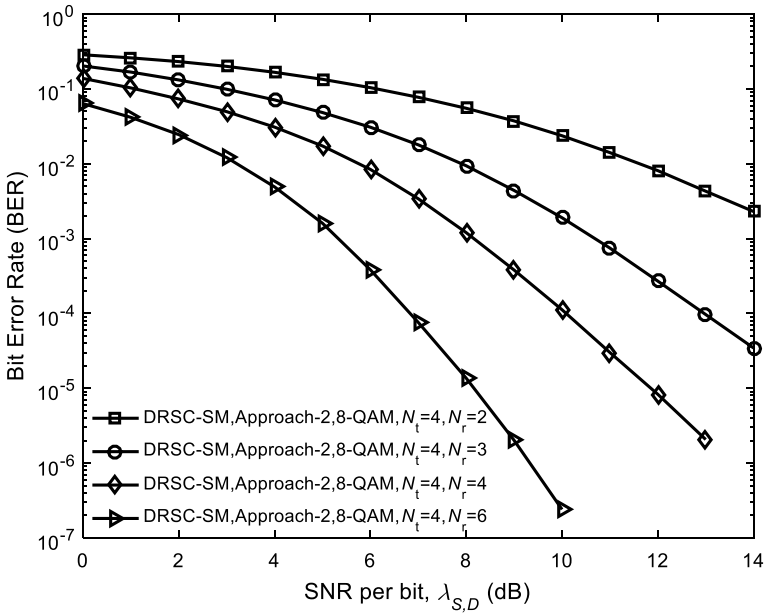

Fig. 15 Performance of DRSC-SM scheme (8-QAM) with various N_r employing $RS_1(31, 25)$ and $RS_2(31, 13)$. The solid line with square mark demonstrates the BER performance of DRSC-SM scheme under $N_r = 2$. The solid line with circle mark demonstrates the BER performance of DRSC-SM scheme under $N_r = 3$. The solid line with diamond mark demonstrates the BER performance of DRSC-SM scheme under $N_r = 4$. The solid line with right triangle mark demonstrates the BER performance of DRSC-SM scheme under $N_r = 6$

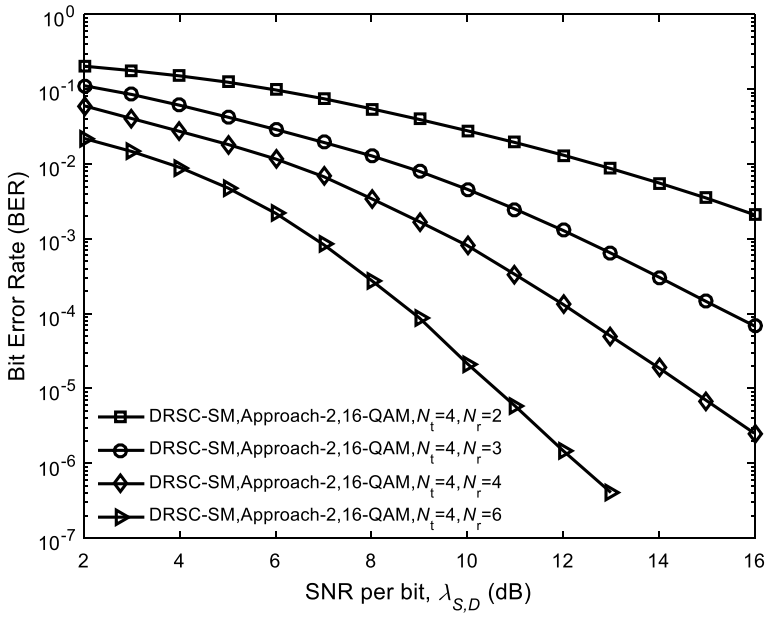

Fig. 16 Performance of DRSC-SM scheme (16-QAM) with various N_r employing $RS_1(63,61)$ and $RS_2(63,41)$. The solid line with square mark demonstrates the BER performance of DRSC-SM scheme under $N_r = 2$. The solid line with circle mark demonstrates the BER performance of DRSC-SM scheme under $N_r = 3$. The solid line with diamond mark demonstrates the BER performance of DRSC-SM scheme under $N_r = 4$. The solid line with right triangle mark demonstrates the BER performance of DRSC-SM scheme under $N_r = 6$

value of N_r adds the spatial diversity in DRSC-SM scheme that will eventually enhance the overall performance of the communication system.

6.5 Performance of the proposed DRSC-SM scheme and the existing schemes

This section compares the performance of the proposed DRSC-SM scheme and the existing schemes, i.e., RS-coded cooperative SM (RSCC-SM) [16] and distributed RS coding (DRSC) [17] under $\lambda_{S,R} = \infty$.

Figure 17 shows the simulation results of the proposed DRSC-SM scheme and the RSCC-SM scheme [16]. The simulation conditions such as $N_t = 4$, 16-QAM, ML detection and smart decoding algorithm are used in the two schemes. Moreover, our proposed scheme adopts the optimized Approach 2 at the relay to get the optimized selection pattern by which partial symbols are selected from the source information symbols for further encoding. However, in the existing RSCC-SM scheme, the relay selects the partial symbols from the source information symbols for further encoding based on the random selection pattern. From Fig. 17, we observe that our proposed DRSC-SM outperforms the existing RSCC-SM. For example, at BER $= 1.4 \times 10^{-4}$, the DRSC-SM scheme with $N_r = 4$ is 0.9 dB better than the RSCC-SM with $N_r = 4$. At the same BER, under $N_r = 6$, the DRSC-SM scheme is 1 dB better than its counterpart. The main reason for such an attractive performance gain is that our proposed DRSC-SM scheme enables to construct a code with a larger minimum distance (i.e., 48) at the destination by appropriately selecting the partial information symbols at the relay.

Figure 18 shows the performance comparison between the proposed DRSC-SM scheme and the existing DRSC scheme [17]. The same conditions such as $RS_1(31,27)$, $RS_2(31,17)$,

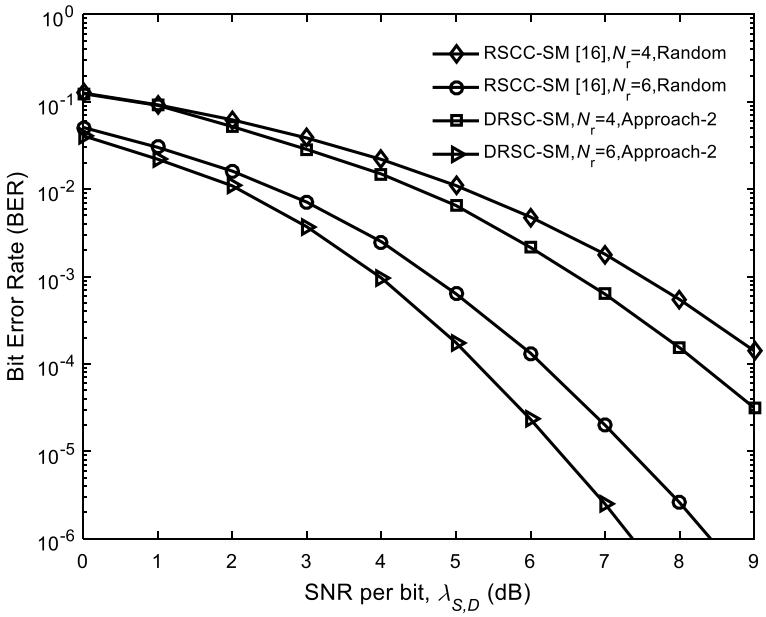

Fig. 17 BER performance of DRSC-SM and RSCC-SM schemes employing $RS_1(63, 51)$ and $RS_2(63, 31)$. The solid line with diamond mark demonstrates the BER performance of RSCC-SM scheme with random selection pattern under $N_r = 4$. The solid line with circle mark demonstrates the BER performance of RSCC-SM scheme with random selection pattern under $N_r = 6$. The solid line with square mark demonstrates the BER performance of DRSC-SM scheme with Approach 2 under $N_r = 4$. The solid line with right triangle mark demonstrates the BER performance of DRSC-SM scheme with Approach 2 under $N_r = 6$

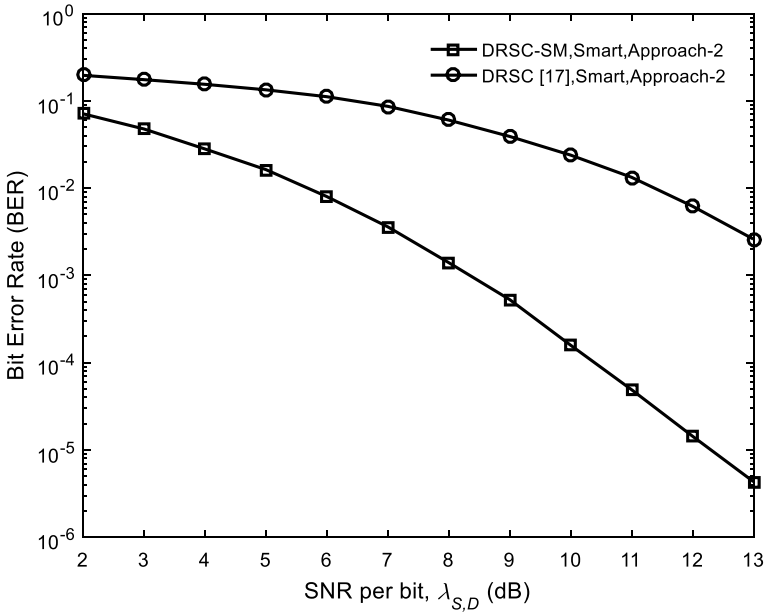

Fig. 18 BER performance of DRSC-SM ($N_t = N_r = 4$ and 8-QAM) and DRSC (32-QAM). The solid line with square mark demonstrates the BER performance of DRSC-SM scheme. The solid line with circle mark demonstrates the BER performance of DRSC scheme

Approach 2, ML detection and smart decoding algorithm are adopted in the two compared schemes. The simulated results in Fig. 18 reflect the superiority of our proposed scheme. For instance, at SNR = 13 dB, the DRSC-SM scheme achieves a very promising performance (i.e., 4.3×10^{-6}) but the DRSC scheme obtains a poor performance (i.e., 2.6×10^{-3}). The performance enhancement is mainly because the adopted novel SM technique provides spatial diversity for the proposed DRSC-SM scheme.

6.6 Performance comparison between DRSC-SM and DRSC-V-BLAST schemes

In Sect. 6.5, Fig. 18 exhibits the performance advantages of our proposed DRSC-SM scheme over the DRSC (without SM). To further confirm the performance superiority of our proposed DRSC-SM scheme, we compare it with the distributed RS-coded V-BLAST (DRSC-V-BLAST) scheme under an identical spectral efficiency. The condition $\lambda_{S,R} = \infty$ is supposed. In our proposed DRSC-SM scheme, $N_t = 4$ and 4-QAM are used. However, $N_t = 2$ and 4-QAM are used in the DRSC-V-BLAST scheme. At the destination, the smart decoding algorithm is used to jointly recover the source information. Moreover, the DRSC-SM scheme utilizes the maximum ratio combining (MRC) reception [20], and the minimum mean squared error (MMSE) detection [20] is adopted in the DRSC-V-BLAST scheme. The significant performance gains of the DRSC-SM scheme over the DRSC-V-BLAST scheme are shown in Fig. 19. For instance, under $N_r = 4$ and 6, 0.5 dB and 0.4 dB gains are obtained by our system at BER=10^{-4}. The main reason behind the attractive gains is that our presented DRSC-SM scheme can completely avoid the drawback (ICI)

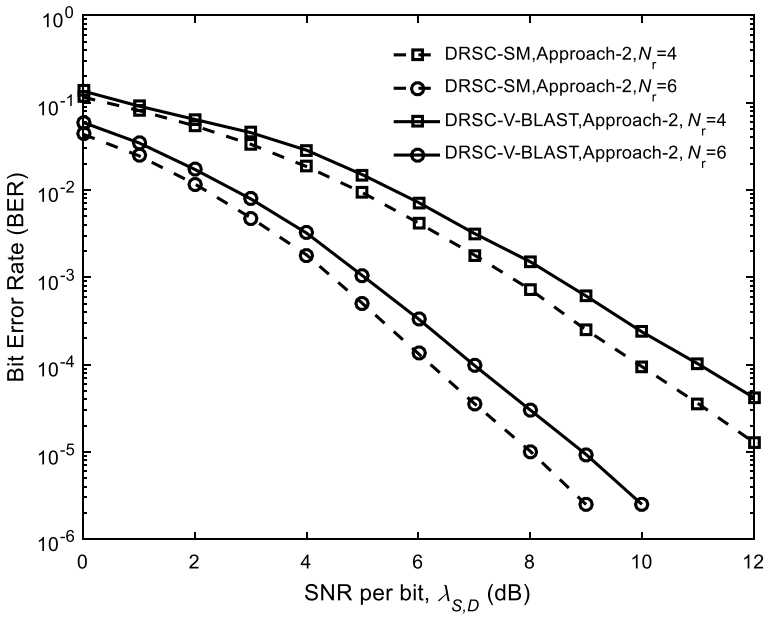

Fig. 19 Performance comparison between the DRSC-SM and DRSC-V-BLAST schemes with $RS_1(15, 13)$ and $RS_2(15, 7)$. The dashed line with square mark demonstrates the BER performance of DRSC-SM scheme under $N_r = 4$. The dashed line with circle mark demonstrates the BER performance of DRSC-SM scheme under $N_r = 6$. The solid line with square mark demonstrates the BER performance of DRSC-V-BLAST scheme under $N_r = 4$. The solid line with circle mark demonstrates the BER performance of DRSC-V-BLAST scheme under $N_r = 6$

of the DRSC-V-BLAST scheme so that the ability to recover the source information is improved.

7 Conclusion

A novel DRSC-SM scheme is proposed. The optimized design approaches are employed for appropriate selection of symbols at the relay node. The numerical results show the effectiveness of the proposed approaches. The destination performs joint RS decoding, which is based on three different algorithms called naive algorithm, smart algorithm and improved smart algorithm. The BER performance curves show that under the same decoding algorithm, the proposed DRSC-SM scheme has an excellent performance over the corresponding coded noncooperative scheme. Also, the DRSC-SM scheme utilizing the improved smart decoding algorithm outperforms the counterpart DRSC-SM scheme using the naive and smart decoding algorithms under identical conditions.

Abbreviations

RS	Reed–Solomon
DRSC-SM	Distributed RS-coded spatial modulation
MIMO	Multiple-input multiple-output
V-BLAST	Vertical Bell Labs Layered Space-Time
IAS	Inter-antenna synchronization
ICI	Inter-channel interference
SM	Spatial modulation
CF	Compress-and-forward
DF	Decode-and-forward
AF	Amplify-and-forward
LDPC	Low-density parity-check
RM	Reed–Muller
BER	Bit error rate
M2M	Machine-to-machine
D2D	Device-to-device
MDS	Maximum distance separable
RF	Radio frequency
ML	Maximum likelihood
SNR	Signal-to-noise ratio
GCD	Greatest common divisor
CRC	Cyclic redundancy check

Acknowledgements
The authors would like to thank the National Natural Science Foundation of China under the contract no. 61771241.

Author contributions
CZ wrote this manuscript. All the authors read and approved the final manuscript.

Funding
The work is supported by the National Natural Science Foundation of China under the contract no. 61771241.

Availability of data and materials
Not applicable.

Declarations

Competing interests
The authors declare that they have no competing interests.

Received: 12 February 2021 Accepted: 1 January 2023
Published online: 09 January 2023

References

1. C. Zhao, F. Yang, R. Umar, Two-source asymmetric turbo coded cooperative spatial modulation scheme with code matched interleaver. Electronics. **9**(1) (2020)

2. R. Govender, N. Pillay, H. Xu, Soft-output space-time block coded spatial modulation. IET Commun. **9**(8), 2786–2796 (2014)
3. R.Y. Mesleh, H. Haas, S. Sinanovic, Spatial modulation. IEEE Trans. Veh. Technol. **57**(4), 2228–2241 (2008)
4. S. Ejaz, F. Yang, Jointly optimized ReedMuller codes for multilevel multirelay coded-cooperative VANETS. IEEE Trans. Veh. Technol. **66**(5), 4017–4028 (2017)
5. S. Mughal, F. Yang, H. Xu, R. Umar, Coded cooperative spatial modulation based on multi-level construction of polar code. Telecommun. Syst. **70**(3), 435–446 (2018)
6. R. Umar, F. Yang, S. Mughal, Multiple relay based Reed Muller network coded cooperation for wireless communication systems. IET Commun. **13**(13), 2034–2044 (2019)
7. S. Ejaz, F. Yang, T.H. Soliman, Multi-level construction of polar codes for half-duplex wireless coded-cooperative networks. Frequenz **69**(11–12), 509–517 (2015)
8. S. Zhang, F. Yang, L. Tang, Joint design of QC-LDPC codes for coded cooperation system with joint iterative decoding. Int. J. Electron. **103**(3), 384–405 (2015)
9. S. Mughal, F. Yang, S. Ejaz, Asymmetric turbo code for coded-cooperative wireless communication based on matched interleaver with channel estimation and multi-receive antennas at the destination. Radioengineering **26**(3), 878–889 (2017)
10. S. Mughal, F. Yang, R. Umar, Reed–Muller network coded-cooperation with joint decoding. IEEE Commun. Lett. **23**(1), 24–27 (2019)
11. J. Kim, J. Lee, J. Kim, J. Yun, M2M service platforms: survey, issues and enabling technologies. IEEE Commun. Surv. Tutor. **16**(1), 61–76 (2014)
12. J. Qiu, L. Chen, S. Liu, A novel concatenated coding scheme: RS-SC-LDPC codes. IEEE Commun. Lett. **24**(10), 2092–2095 (2020)
13. A.H. Almawgani, M.F. Salleh, RS coded cooperation with adaptive cooperation level scheme over multipath Rayleigh fading channel, in *Proceedings of IEEE 9th Malaysia International Conference on Communications (MICC)* (IEEE Kuala Lumpur, Malaysia, 2009), pp. 480–484
14. A.H. Almawgani, M. Salleh, Coded cooperation using Reed Solomon codes in slow fading channel. IEICE Electron. Express **7**(1), 27–32 (2010)
15. Y.M. Al-moliki, M.A. Aldhaeebi, G.A. Almwald, M.A. Shaobi, The performance of RS and RSCC coded cooperation systems using higher order modulation schemes, in *Proceedings of 6th International Conference on Intelligent Systems, Modelling and Simulation.* (IEEE Kuala Lumpur, Malaysia, 2015), pp. 211–214
16. C. Zhao, F. Yang, D.K. Waweru, Reed–Solomon coded cooperative spatial modulation based on nested construction for wireless communication. Radioengineering **30**(1), 172–183 (2021)
17. P. Guo, F. Yang, C. Zhao, W. Ullah, Jointly optimized design of distributed Reed-Solomon codes by proper selection in relay. Telecommun. Syst. **78**(3), 391–403 (2021)
18. M. Koca, H. Sari, Bit-interleaved coded spatial modulation, in *IEEE 23rd international symposium on personal indoor and mobile radio communications* (IEEE Sydney, Australia, 2012), pp. 1949–1954
19. L. Shu, S. Lin, D.J. Costello, *Error Control Coding* (Pearson Education India, 2004)
20. J.R. Barry, E.A. Lee, D.G. Messerschmitt, *Digital Communication* (Springer, New York, 2004)

Publisher's Note

Springer Nature remains neutral with regard to jurisdictional claims in published maps and institutional affiliations.